Weather and Climate Extremes 47 (2025) 100753

Contents lists available at ScienceDirect

Weather and Climate Extremes

journal homepage: www.elsevier.com/locate/wace

# Projected changes in daily temperature extremes for selected locations over South Africa

Charlotte M. McBride [a,b,*], Andries C. Kruger [a,b], Charmaine Johnston [c], Liesl Dyson [b]

[a] South African Weather Service, Climate Service Department, Pretoria, South Africa
[b] Department of Geography, Geoinformatics and Meteorology, Faculty of Natural and Agricultural Sciences, University of Pretoria, Pretoria, South Africa
[c] Council for Scientific and Industrial Research (CSIR), Pretoria, South Africa

ARTICLE INFO

*Keywords:*
Climate projections
Scenarios
Extreme temperatures
CORDEX
Return periods
South Africa

ABSTRACT

Extreme events, particularly very high temperatures, are expected to increase because of climate change. It is thus essential that localised studies be done to quantify the magnitude of potential changes so that proper planning, especially effective adaptation measures, can be affected. This study analysed annual extreme daily maximum temperatures for future climate change scenarios at 22 locations in South Africa, through analysis of a subset of the Coordinated Regional Downscaling Experiment (CORDEX) model ensemble datasets. The multi-model simulations were validated against observational data obtained from the South African Weather Service for the period 1976–2005. Two study periods of mid- (2036–2065) and far-future (2066–2095) were analysed for two Representative Concentration Pathways, i.e., RCP4.5 and RCP8.5. Bias correction was done on the model data to correct simulated historical climate data, to be more characteristic of observed measurements. While the method included adjustment for variance, systematic underestimations of extremes were still evident. The Generalized Extreme Value distributions were fitted to the bias-corrected projections, and 10-, 50- to 100-year return periods quantile values were estimated. The return period quantile values are likely to increase under both Representative Concentration Pathways in the mid- and far-future periods, with the largest increase in return period quantile values set to occur towards the end of the century under the highest emission scenario. All stations showed an increase in the frequency of days with maximum temperatures above specific critical thresholds, with some stations under the RCP8.5 scenario projected to experience temperatures of greater than 32°C (35°C) for more than 200 (100) days per year by the end of the century, an increase from a baseline of approximately 70 to 150 (14 to 83). For the same scenario, Return periods for 38°C for most stations are projected to be shorter than a year. From the above and considering the likely underestimation in the severity of the projected changes, i.e. too low return period quantile values, the general implication is a strong likelihood that most places in South Africa is likely to experience a strong increase in the intensity, duration, and frequency of very hot extremes in future, with potentially dire consequences to relevant socio-economic sectors. We suggest that future research, comprised of the full set of CORDEX data be conducted to optimise the results of this study.

## 1. Introduction

As the global climate is warming, it is expected that the intensity and frequency of climatic extremes are likely to be affected (Fischer and Knutti, 2014; Saddique et al., 2020). These changes in extreme events are likely to have a larger impact on human health and natural systems compared to the expected changes in the mean climate (Katz and Brown, 1992).

According to the IPCC Working Group I contribution to the Sixth Assessment Report (Arias et al., 2021), the mean global temperatures have increased by 1.09 °C (0.95 °C–1.2 °C) during the period 2011 to 2020 since the preindustrial period of 1850–1900. The IPCC's Working Group I contribution to the Fifth Assessment Report, which was the last IPCC report to use Representative Concentration Pathways (RCPs), highlights that the global mean surface temperatures are "likely" to show a projected increase of more than 1.5 °C relative to the preindustrial period if the world continues to follow an RCP of 4.5, and "high confidence" to occur at RCP8.5. There is also "high confidence" that it's likely that global mean temperatures above 2 °C, will be reached for RCP8.5 by the end of the century (IPCC, 2013). The IPCC's Working

* Corresponding author. South African Weather Service, Private Bag X097, Pretoria, 0001, South Africa.
*E-mail address:* charlotte.mcbride@weathersa.co.za (C.M. McBride).

https://doi.org/10.1016/j.wace.2025.100753
Received 23 October 2023; Received in revised form 13 January 2025; Accepted 11 February 2025
Available online 13 February 2025

Group I contribution to the Sixth Assessment Report also goes on to state that there is now "high confidence" that the frequency of hot extremes has increased globally.

With Africa projected to warm at a higher rate than the global average (Engelbrecht et al., 2015; Nangombe et al., 2019), and with its low resilience and limited adaptive capacity (Fotso-Nguemo et al., 2023) and large reliance on rain-fed agriculture (Serdeczny et al., 2017), it is essential that changes in climate extremes are researched at a local level. Many studies have shown that hot extreme events have serious consequences for human, animal and crop health in the African context (Maluleke and Mokwena, 2017; Wichmann, 2017; Chersich et al., 2018; Hlahla and Hill, 2018; Mafongoya et al., 2019; Olabanji et al., 2020), compared to more-developed parts of the world. In terms of human health, there have been studies done on increases in child mortality rates (Chapman et al., 2022), heat stress (Garland et al., 2015; Fotso-Nguemo et al., 2023), increase in cardiovascular disease (Bühler et al., 2022), and increases in hospital admissions (Makunyane et al., 2023), all due to hot extremes. These temperature-related mortality impacts are very dependent on a wide range of socioeconomic and physiological factors (Asefi-Najafabady et al., 2018), and thus the local context needs to be considered. Research into agricultural production has also noted the adverse effects of temperature extremes, which include, for example, cattle reducing their feed intake when temperatures exceed 35 °C (Blackshaw and Blackshaw, 1994), implying less milk production and a general deterioration in animal health (Morrison, 1983; Bohmanova et al., 2007). High temperatures during specific developmental stages of plant growth for crops such as wheat, maize and rice can significantly reduce yields (Rosenzweig et al., 2001; Sarr et al., 2019). In the developing world, this was equated to a 2.66 % lower growth in agricultural output for every 1 °C increase in temperature (Dell et al., 2012). Other impacts include more frequent, longer and more intense heat waves (Mbokodo et al., 2020, 2023), changes in vector-borne disease outbreak patterns (Anyamba et al., 2014), increase in armed conflict (Burke et al., 2009) and increase in fire-danger days (Engelbrecht et al., 2015), amongst others. As all these impacts are related to hot extremes, the expected increases thereof, rather than in the mean temperature, are more likely to affect society (Hegerl et al., 2004).

Studies have shown that both the trend in mean annual temperature (Collins, 2011; MacKellar et al., 2014; Kruger and Nxumalo, 2016) and hot extremes (New et al., 2006; Kruger and Sekele, 2013; Kruger et al., 2019, 2020; McBride et al., 2021; Van Der Walt and Fitchett, 2021) for South Africa has been positive with the rate of change increasing in recent decades. In terms of future projections, Almazroui et al. (2020) found that according to temperature projections over different African regions using the CMIP6 ensemble of models, temperatures are projected to increase over the eastern parts of South Africa from the present climate (1981–2010) under the RCP4.5 and RCP8.5 scenarios during the period 2030–2059 (2070–2099) by 1.4 (2.3)°C and 1.7 (4.1)°C respectively. Over the western parts of the country for the same periods and RCPs, projected increases of 1.6 (2.7)°C and 1.9 (4.7)°C are expected. The median projection of change in annual maximum temperatures from the Coordinated Regional Climate Downscaling Experiment (CORDEX) data for a similar period of 2080–2099 but compared to a current climate of 1971–2000 conducted by Archer et al. (2018) showed an increase of about 3 °C for RCP4.5–5 °C for RCP8.5 for the interior of the country, while coastal stations showed 1.5–2 °C less of an increase.

A study by Hegerl et al. (2004) showed that it is possible to detect anthropogenic influences on extreme temperatures by examining the trend thereof. Model projections such as those from the CORDEX (https://cordex.org/domains/region-5-africa/) are suitable tools for looking at climate variability and change (Endris et al., 2013; Iturbide et al., 2022). These models are the primary tools for studying possible future climate changes (Kharin et al., 2005) and can thus provide estimates for future extreme temperature changes.

This paper will focus on likely changes in the probabilities of future hot temperature extremes for 22 locations with homogeneous temperature time series over the CORDEX simulation period across South Africa. This type of research may assist in the mitigation and management of these types of extreme events (Zwiers et al., 2011; Frías et al., 2012; Kuang et al., 2021; Lee et al., 2020), through evidence-based planning and preparedness (Turasie, 2021).

We use projected future changes in the occurrence of daily maximum temperatures above pre-defined thresholds, return period quantile values for specified return periods (RPs), and likely future changes in RPs of extreme temperatures from that expected in the current-day climate. Probability estimations are done by application of the Generalized Extreme Value (GEV) distribution, which has also been used by Kharin and Zwiers (2005), Kharin et al. (2007, 2013), Kuang et al. (2021) and Turasie (2021) in related studies. However, it should be noted that uncertainties exist due to the differences in ensemble members in such a study, which is addressed in the discussion of Fig. 2. By estimating RPs of specific magnitudes, one can estimate probabilities of occurrences of these events and be in a better position to plan for adaptation interventions (Almazroui et al., 2021; Turasie, 2021). Therefore, understanding these changes will enable better local preparedness and assist in developing the necessary policy interventions (Ziervogel and Zermoglio, 2009).

The paper is set out with an introduction in Section 1, followed by a discussion of the data and methods, including bias correction, in Section 2. Results are presented in Section 3, while Section 4 discusses the results and summarises the implications.

## 2. Data and methods

### 2.1. Representative Concentration Pathways

When considering climate change, it makes sense to use a common set of scenarios or RCPs, which contain air pollution emission, greenhouse gas concentration and land use trajectories (Van Vuuren et al., 2011). This study considers two of these pathways: the intermediate scenario RCP4.5 with radiation forcing levels of 4.5W/m$^2$, where emissions peak around 2040 and then decline. The second is the RCP8.5, with radiation forcing levels of 8.5W/m$^2$, where emissions are not expected to decrease throughout the 21st century (Meinshausen et al., 2011).

### 2.2. Data and methods

Model data was obtained from the CORDEX (https://cordex.org/domains/region-5-africa/) and in the form of dynamically downscalling to a 0.44° horizontal resolution produced by the Rossby Centre Regional Model (RCA4), a climate modelling research unit at the Swedish Meteorological and Hydrological Institute. The model data was forced across its lateral boundaries by nine Atmosphere-Ocean General Circulation Models (AOGCMs) (Table 1), run under the Climate Model Intercomparison Project Phase 5 https://pcmdi.llnl.gov/mips/cmip5/. CMIP is an ongoing project of the World Climate Research Program (WCRP). Although CMIP6 model runs are already available (https://cds.

**Table 1**
Projections from nine Atmospheric-Ocean General Circulation Models used in this study, after downscaled by RCA4.

| Model | Institute (country) | Reference |
|---|---|---|
| A. CanESM2m | CCCMa (Canada) | Arora et al. (2011) |
| B. CNRM-CM5 | CNRM-CERFACS (France) | Voldoire et al. (2013) |
| C. CSIRO-Mk3 | CSIRO-QCCCE (Australia) | Rotstayn et al. (2013) |
| D. IPSL-CM5A-MR | IPSL (France) | Hourdin et al. (2013) |
| E. MICRO5 | AORI-NIES-JAMSTEC (Japan) | Watanabe et al. (2011) |
| F. HadGEM2-ES | Hadley Centre (UK) | Hirabayashi et al. (2013) |
| G. MPI-ESM-LR | MPI-M (Germany) | Ilyina et al. (2013) |
| H. NorESMI-M | NCC (Norway) | Tjiputra et al. (2013) |
| I. GFDL-ESM2M | GFDL (USA) | Dunne et al. (2012) |

climate.copernicus.eu/cdsapp#!/dataset/projections-cmip6?tab=overview), the CORDEX downscaling thereof is still being planned (https://wcrp-cordex.github.io/simulation-status/CORDEX_CMIP6_status.html), therefore this study still utilizes CIMP5-based model data. Historical simulations were created for the period 1976–2005 (current climate), while the projected data sets cover two future periods, i.e., mid- (2036–2065) and far-future (2066–2095). The historical simulations were compared to near-surface daily South African Weather Service's temperature data at 22 locations (Fig. 1). The data were quality controlled and homogenized (Kruger et al., 2019), and is a dataset used by the South African Weather Service for ongoing research and monitoring of mean and extreme temperature trends and records over South Africa (Kruger and Nxumalo, 2017; McBride et al., 2021). The trigonometrical estimation method was used to estimate the model surface temperature at each station's location (Kruger et al., 2019).

The historical simulations and future projections of the nine AOGCMs downscaled by RCA4 were considered for calculating the probabilities in hot extreme temperatures. These subset of nine models outputs was also applied by Kruger et al. (2019). Their study compared the consistencies of the model-simulated trends against the associated observed trend and suggested that the models were able to simulate the average trend based on observations. Therefore, the same model outputs were used in this paper as well. This study used one CORDEX regional climate model and thus the results are considered to be 'model dependent'. However, regardless of the evaluations of the model simulations, it should be noted that in Kruger et al. (2019) and here, the complete set of CORDEX of more than 20 outputs were not utilized, and therefore cannot be considered to be better-performing than the entire CORDEX ensemble. Therefore, the results cannot be considered optimal but still provide an indication of the scale of increases in the probabilities of future hot extremes. Future studies might like to consider other regional models to see if they provide similar findings and help to better describe the uncertainties associated with the projections, after evaluation of model simulations with observations.

Following on the above, comparison between the observed and simulated trends emphasizes the necessity to assess the reliability of the output of climate models which have a bearing on the credibility of projections. This suite of selected models has been used in previous studies (Botai et al., 2020; Kruger et al., 2019) and has been verified against actual observations at the locations of interest (Kruger et al., 2019). In Kruger et al. (2019), this critical point comparison between observed and downscaled model-simulated time series provides valuable information regarding the interpretation of model-generated projections. One important finding relevant to this research is that the model simulations, on average, for annual average and extreme maximum temperatures, showed more consistency in increases than the observations between station locations. We can, therefore, assume with a measure of confidence, that the projected extreme temperatures on which this analysis is based, will be biased towards more conservative values, i.e. projection estimates that are biased to rather overestimate than underestimate projections of high extremes in temperature. Thus, this limitation of the models to effectively simulate the range of observed climate extremes (especially the cases at locations with lower trends) renders the projections conservative, which is an important result in the light of climate change adaptation. This critical comparison of observations vs. model simulations is considered vital in confident model selection (Nguyen et al., 2024).

The approach for the study was to take the annual highest daily maximum temperatures for the observed and the model data for each location and compare these for a common historical period of 1976–2005 to check for systematic errors in the models. Bias correction was then done to align the model data with the observations for each station. These corrections were then applied to the two projection periods of 2036–2065 (mid-) and 2066–2095 (far-futures). Alignment between annual maxima of the observations and model simulations were tested with the Kolmogorov–Smirnov (K-S) test at the 5% significance level. The rate of occurrence and probability of occurrence were investigated for a range of pre-defined extreme temperature thresholds. The study then looked at the future potential risk of an extreme temperature by investigating the average number of days above these critical temperatures for all models for the RCP4.5 and RCP8.5 scenarios for the mid- and far-futures. The average interval period between events,


**Fig. 1.** Locations of the 22 climate stations with long-term homogeneous temperature time series across South Africa, which were used in the analysis.

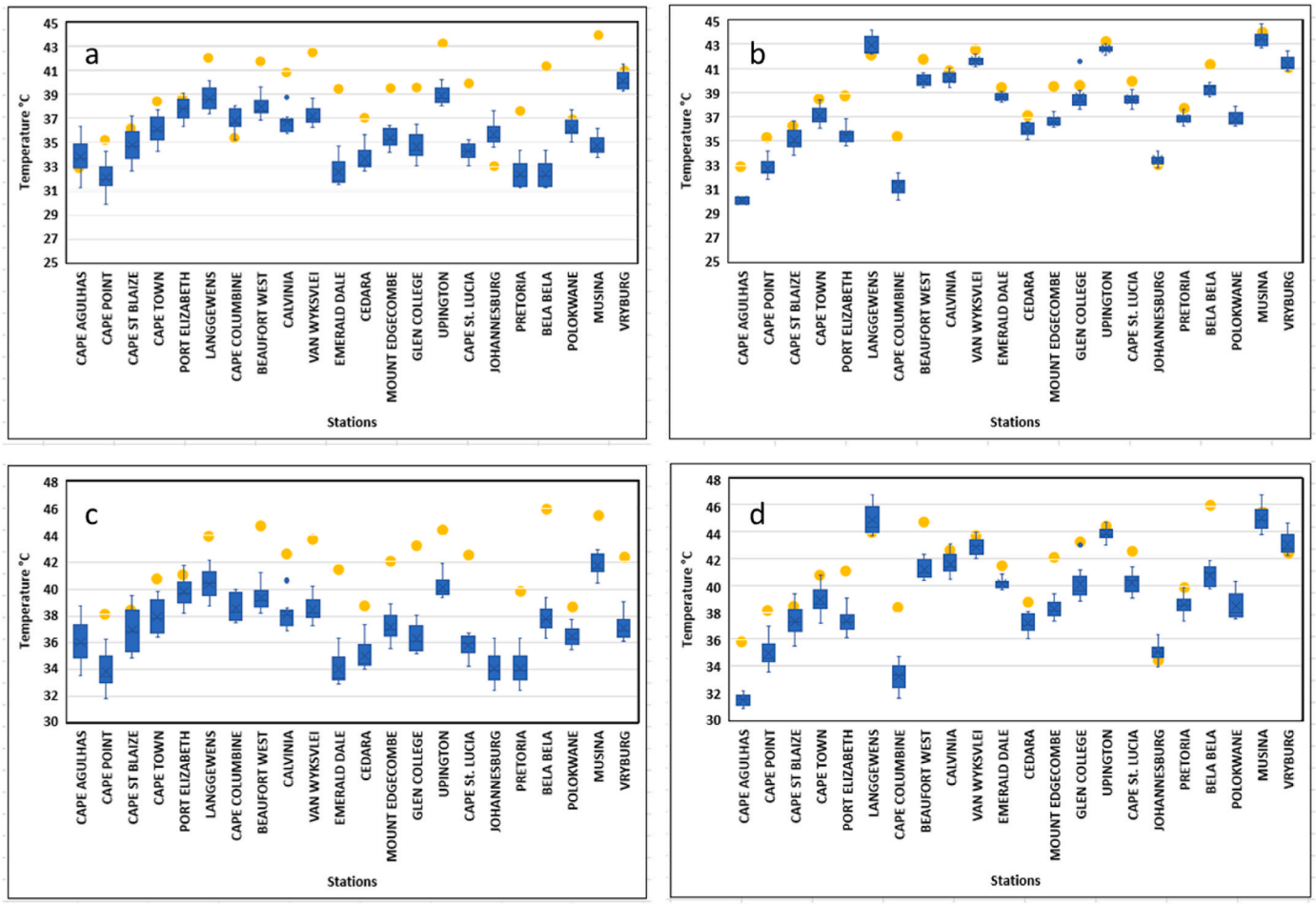


**Fig. 2.** Box-and-whisker plots from all models for 10- and 50-year return period quantile values. Graphs a and c are obtained from the non-bias-corrected data for 10- and 50-year, respectively, while b and d are from the bias-corrected data for 10- and 50-year, respectively. The bottom and top of the blue boxes in the graphs show Quartile 1 and 3. The minimum models' value is the bottom whisker, and the top whisker is the maximum models' value. The models' median is shown with the line in each box. The floating blue points show outliers. The observed return period quantile values are shown with yellow dots.

referred to as return periods (RPs), was estimated. The future RPs of the current return period quantile values (the extreme value associated with a specific RP), given the projected extreme value distribution parameters from the RCP4.5 and RCP8.5 for the mid-and far-future scenarios, were also determined.

### 2.2.1. Bias correction

A trend-preserving bias correction method developed by the Inter-Sectoral Impact Model Intercomparison Project (ISI-MIP) (Hempel et al., 2013) was applied to the CORDEX dataset. The method preserves the absolute changes/trends in monthly temperature, which is followed by correction of the daily variability about the monthly mean. Therefore, the data is divided into months, and the monthly mean and variance are corrected by constant offsets and multiplicative correction factors. Thus, the whole data sets were corrected, not just the extreme values, and by correcting the mean and variance biases, the extreme values may then be improved (Xu et al., 2021). The correction factors are derived from the observational data and the simulated data for all nine models for the common period 1976 to 2005.

#### 2.2.1.1. Mean offset for each month

$$C = \left( \sum_{i=1}^{n=30} T_{iObs} - \sum_{i=1}^{n=30} T_{iModel} \right) \Big/ 30 \tag{1a}$$

The correction for each month's daily temperature is then:

$$\widetilde{T}_{ij}^{model} = C + T_{ij}^{model} \tag{1b}$$

$i$ = specific year
$j$ = particular day.

#### 2.2.1.2. Variance correction.

To correct the variability of the daily average temperature values to the observational data, we adjust the residual distribution of the GCM to that of the observations using parametric quantile mapping. In general, temperature values follow a normal distribution. This means the distribution is expected to be well described by only two moments (mean and standard deviation). For that reason, a linear fit is considered an appropriate approximation in most cases and has thus been chosen to map the simulated to the observational temperature values (Hempel et al., 2013).

$$f(\Delta T_{Model}) = B \,.\, \Delta T_{Model} \tag{1c}$$

$B$ is the slope of the linear regression on the rank ordered *Obs* ($\Delta T_{Obs}$) and *Model* data ($\Delta T_{Model}$) for a given month over the common 30-year period. The constant offsets and multiplicative correction factors are then applied to the simulated projection data. Hempel et al. (2013) found the width (and skewness) of the distribution of the daily averaged temperature values shows good agreement between the observational and bias-corrected model data, through inspection of the interpercentile ranges between the two data sets. Also, on the global scale the bias-corrected variables show good agreement with the observational

data even in the tails of the distribution, which is the focus of this study (Hempel et al., 2013).

The K-S goodness-of-fit test was used to validate the bias correction method. Such approaches have been used in similar studies (Ahmadalipour et al., 2017; Xu et al., 2017; Lim Kam Sian et al., 2022). This nonparametric test quantifies the maximum distance between the empirical distribution functions derived from two different samples of data; in this case, the observed and the model data (Lanzante, 2021). The 5% significance level was chosen; thus, if the *p*-value is larger than 0.05, the null hypothesis is accepted that the samples are drawn from the same distribution. The statistic is defined as follows (Lim Kam Sian et al., 2022):

$$D_{n,m} = \max \left| Obs_n(TXx) - Model_m(TXx) \right| \quad (2)$$

$D$ = maximum distance between the empirical distribution functions.
*Obs* = observational data.
*Model* = simulated data
$n$ and $m$ = the number of elements for observational and model data respectively.
*TXx* = highest annual maximum temperature.

The effect of correcting the variance was not fully explored in terms of the distribution shapes of the tail of the distribution before and after the bias correction. However, the addition of the correction for variance is expected to render overestimated rather than underestimated extreme values and thus provides more conservative estimates of RPs. Here, "conservative" means to be biased towards overestimation of return period quantile values, which is a more careful or prudent approach with regards to forward planning. Therefore, the implication of the adopted bias correction procedure on the results of the analyses of future change in return period of events of particular magnitudes would be a bias towards shorter periods.

#### 2.2.2. Critical values

Based on the literature, certain daily maximum temperatures were viewed as critical thresholds.

- +35 °C - causes severe loss to crop yields for maize and wheat (Zhu and Troy, 2018) and cattle reduce their feed intake and dairy cows reduce their milk production (Morrison, 1983; Blackshaw and Blackshaw, 1994; Bohmanova et al., 2007),
- +32 to +38 °C - strong heat stress, +38 to +46 °C - very strong heat stress and >46 °C - extreme heat stress in humans (Bröde et al., 2012)

A count of daily maximum temperatures from all models for each station above 32 °C, 35 °C, 38 °C and 46 °C was made and averaged on an annual basis to quantify the projected annual frequency of temperatures above these thresholds in the mid-and far-futures under RCP4.5 and RCP8.5, compared to the current-day climate.

#### 2.2.3. Extreme value analysis

The GEV model was applied to estimate the probabilities of extreme events (Kim Yeon-Hee et al., 2020), using best-fit distribution for analyzing extreme maximum temperatures (Ng et al., 2022). Annual maximum temperatures for each station for both observed and model outputs were used as the series of independent observations to which the GEV distribution was fitted by the method of *L* moments (Hosking, 1990).

The GEV is defined as:

$$F(x) = e^{-(1-ky)^{1/k}} \; k \neq 0 \quad (3.1a)$$

$$F(x) = e^{-e^{(-y)}} \quad k = 0 \quad (3.1b)$$

$k$ = shape parameter (determines the type of extreme value distribution).
$y$ = standardised or reduced variate.

When $k = 0$, the GEV is an Extreme Value Distribution Type I (Gumbel).

The standardized or reduced variate $y$ is given by:

$$y = (x - \beta)/\alpha \quad (3.2)$$

$\alpha$ = scale or dispersion parameter
$\beta$ = mode of the extreme value distribution
$x$ = the extreme value

To estimate $\alpha$ and $\beta$ we used the method of moments (Wilks, 2011):

$$\alpha = s\sqrt{6}\Big/\pi \quad (3.3)$$

$$\beta = \overline{x} - \gamma\alpha \quad (3.4)$$

$s$ = standard deviation of sample
$\overline{x}$ = sample mean
$\gamma$ = 0.57721 … Euler's constant.

The focus was on 10 year return period quantile values as a measure of more immediate outcomes, whereas the 50- and 100-year values provided a metric of more exceptional extremes of temperature (Xu et al., 2018). This study averaged the return period quantile values from the participating models that passed the K-S test to give each station a "mean model" value (Alexander and Arblaster, 2009, 2017). This "mean model" value can thus be considered the consensus of the direction of change by the ensemble of models. CORDEX model evaluations have shown that using mean model values is preferable as they outperform individual models (Soares et al., 2019), but again it should be emphasized here that only a sub-set of CORDEX models were utilized. Box-and-whisker plots are used to illustrate the interquartile model ranges for the 10- and 50-year return period quantile values. This indicates the spread of values obtained from the various models.

In addition, the annual maximum temperature return period quantile values for 10-, 50- and 100-years, based on the recent period (1976–2005), were then used together with the location and scale parameters of the future scenarios to calculate the future RPs for these particular current-day return period quantile values:

$$x = \frac{1}{e^{\left(\frac{\beta - TX_m}{\alpha}\right)}} \quad (4)$$

$\alpha$ = location parameter
$\beta$ = scale parameter.
$TX_m$ = mean model return period quantile value.

## 3. Results

### 3.1. Validation of bias-corrected hot annual extreme simulations

In Fig. 2, box-and-whisker plots illustrate how well the bias-corrected model temperatures represented the 10- and 50-year return period quantile values per station compared to the same return period quantile values calculated from the observed temperatures for the period of 1976–2005. The respective observed 10- and 50-year return period quantile values per station are shown as yellow dots on the graph, with the desired outcome to be inside the associated box-and-whisker plots. The bias-corrected temperatures have more stations where the observed return period quantile values have their values within their box-and-whisker plots (Fig. 2b and d) compared to the non-bias-corrected data (Fig. 2a and c). Most stations show that the bias-corrected data are closer to the observed data values (Fig. 2b and d) than before bias correction. However, some notable exceptions exist at Cape Agulhas, Port Elizabeth and Cape Columbine, where the non-biased corrected model temperatures were closer to the observations than the bias-corrected temperatures. This could be due to the 30-year reference period not being adequate in enabling the variability at these individual stations to be adequately sampled (Hempel et al.,

2013), but more so that the models are not effective in simulating the very high extremes that occur from time to time due to off-shore flow (Jury, 1985; Schumann and Martin, 1991). From the results in Fig. 2, and supported by (Kruger et al., 2019), the RCM models are able to capture the principal tenets of mean and extreme temperatures over South Africa. While there is a systematic underestimation of multi-year extremes derived from the model simulations (Fig. 2 a and c), particularly for locations in the interior, the regional variations of the derived figures largely reflect those derived from the observational data.

The underestimation of the observed 10-year return period quantile values meant that stations such as Port Elizabeth and Cape Columbine (Cape Agulhas and Mount Edgecombe) estimated the 10-year return period quantile values to be 3.2 °C and 4.1 °C (both, 2.8 °C) lower than the observed return period quantile values. The interior stations showed less of a discrepancy between model mean and observed return period quantile values, with stations like Vryburg, Johannesburg and Langgewens even having slightly higher return period quantile values of 0.5 °C, 0.4 °C and 1.0 °C, respectively, as compared to the observed return period quantile values. This underestimation of return period quantile values was also seen in the 50-year values with coastal stations such as Cape Columbine, Cape Agulhas, Mount Edgecombe and Port Elizabeth recording return period quantile values of 5.1 °C, 4.2 °C, 3.7 °C and 3.6 °C, respectively below the observed 50-year return period quantile values. Interior stations like Glen College, Beaufort West and Bela Bela also recorded below the observed 50-year return period quantile values by 2.9 °C, 3.3 °C and 5.1 °C. The reason the models are not always able to represent observational return period quantile values well is probably due to the coarse resolution of the models compared to point measurements from observations (Iturbide et al., 2022). Complex topography and boundaries between land and sea can also lead to large uncertainties and biases in simulating extreme events (Giorgi, 2019). Despite the above discrepancies between the observations and the model simulations, there was general agreement among the simulations from the models regarding increases in return period quantile values. Detailed K-S test results, presented in Table 2, indicate, in general, an improved fit for individual models after bias correction in terms of hot annual extreme values. A total of 9% of the models passed the K-S test before bias correction, compared to 66% after bias correction.

Only the models that passed the K-S test were used and averaged for each station to calculate return period quantile values and RPs. For example, Cape Point had only one model (CSIRO-Mk3) deemed acceptable by the K-S test for results from GEV analysis after bias correction, and thus, this was the only model considered for the calculation of return period quantile values and RPs for this station. Three stations (Port Elizabeth, Cape Columbine and Mount Edgecombe) did not have any of their models pass the K-S test at the 5% level, and thus their RPs and return period quantile values were not estimated. However, these stations did have models which passed the K-S test before bias correction, but further investigation showed that the relatively higher variance of these datasets affected the bias correction procedure in such a way as to decrease the correlation between the observations and simulations. Therefore, these stations' data were not used to calculate the RPs and return period quantile values due to the risk of underestimation of projected extreme temperature statistics. Other

**Table 2**
K-S results for validation of bias-corrected annual maximum temperature simulations for each model per station: Red: Reject, Black: Accept hypotheses at the 5% level.

| Model name / Station name | CanESM2m | CNRM-CM5 | CSIRO-Mk3 | IPSL-CM5A-MR | MICRO5 | HadGEM2-ES | MPI-ESM-LR | NorESMI-M | GFDL-ESM2M |
|---|---|---|---|---|---|---|---|---|---|
| Cape Agulhas | 0.07 | 0.01 | 0.13 | 0.07 | 0.04 | 0.04 | 0.04 | 0.07 | 0.02 |
| Cape Point | 0.01 | 0.00 | 0.13 | 0.02 | 0.00 | 0.00 | 0.00 | 0.00 | 0.00 |
| Cape St. Blaize | 0.39 | 0.00 | 0.80 | 0.24 | 0.24 | 0.00 | 0.00 | 0.01 | 0.00 |
| Cape Town | 0.59 | 0.04 | 0.59 | 0.59 | 0.13 | 0.01 | 0.39 | 0.07 | 0.07 |
| Port Elizabeth | 0.00 | 0.00 | 0.00 | 0.02 | 0.00 | 0.00 | 0.00 | 0.00 | 0.00 |
| Langgewens | 0.00 | 0.39 | 0.02 | 0.07 | 0.39 | 0.13 | 0.04 | 0.13 | 0.13 |
| Cape Columbine | 0.00 | 0.00 | 0.00 | 0.00 | 0.00 | 0.00 | 0.00 | 0.00 | 0.00 |
| Beaufort West | 0.07 | 0.04 | 0.59 | 0.80 | 0.39 | 0.39 | 0.04 | 0.00 | 0.24 |
| Calvinia | 0.80 | 0.39 | 0.95 | 0.80 | 0.95 | 0.59 | 0.07 | 0.59 | 0.80 |
| Vanwyksvlei | 0.01 | 0.00 | 0.04 | 0.13 | 0.13 | 0.01 | 0.04 | 0.07 | 0.04 |
| Emerald Dale | 0.23 | 0.80 | 0.24 | 0.39 | 0.80 | 0.39 | 0.80 | 0.59 | 0.80 |
| Cedara | 0.01 | 0.13 | 0.00 | 0.59 | 0.07 | 0.07 | 0.80 | 0.07 | 0.39 |
| Mount Edgecombe | 0.00 | 0.04 | 0.00 | 0.00 | 0.00 | 0.00 | 0.00 | 0.00 | 0.00 |
| Glen College | 0.24 | 0.24 | 0.04 | 0.24 | 0.24 | 0.24 | 0.24 | 0.00 | 0.07 |
| Upington | 0.04 | 0.07 | 0.04 | 0.39 | 0.13 | 0.01 | 0.13 | 0.04 | 0.13 |
| Cape St. Lucia | 0.04 | 0.13 | 0.80 | 0.24 | 0.24 | 0.59 | 0.59 | 0.07 | 0.59 |
| Vryburg | 0.07 | 0.13 | 0.95 | 0.80 | 0.04 | 0.95 | 0.80 | 0.07 | 0.80 |
| Johannesburg | 0.13 | 0.39 | 0.80 | 0.80 | 0.39 | 0.80 | 0.59 | 0.59 | 0.80 |
| Pretoria | 0.24 | 0.80 | 0.80 | 0.80 | 0.95 | 0.39 | 0.80 | 0.95 | 0.39 |
| Bela Bela | 0.39 | 0.39 | 0.39 | 0.13 | 0.59 | 0.07 | 0.59 | 0.59 | 0.59 |
| Polokwane | 0.13 | 0.95 | 0.24 | 0.39 | 0.95 | 0.24 | 0.39 | 0.80 | 0.59 |
| Musina | 0.39 | 0.80 | 0.07 | 0.07 | 0.39 | 0.39 | 0.80 | 0.59 | 0.59 |

stations had variable results, but it is evident that the bias correction was more successful with interior stations than those closer to the coast in terms of annual maximum temperatures.

### 3.2. Critical temperature analysis

For the critical temperature analysis, we examined all stations in the study, regardless of whether the station passed the K-S test. This was because counts of these critical temperatures were compared for each station's observed and projected model runs, and thus not fundamentally relevant whether the specific stations passed the K-S test. When considering critical temperatures (Table 3) as defined in Section 2.2.2, under the two RCPs, the number of days above these critical temperature thresholds will become more frequent during the 2036–2095 period for all stations except for Cape Agulhas. For daily maximum temperature of 32 °C and above, only four stations (Vanwyksvlei, Vryburg, Upington and Musina) recorded more than 100 days a year in the current climate (Table 3: grey column). The number of stations predicted to receive 100 days or more daily maximum temperature of 32 °C and above will increase to six stations for the mid-future, further increasing to eight stations in the far future under RCP4.5. If the RCP8.5 pathway is followed, 13 stations are projected to experience an average of 100 days per year above 32 °C in the far future. Under RCP8.5 by the end of the century, all stations except Cape Agulhas, are projected to experience temperatures of above 32 °C at least once a year, with five stations (Glen College, Bela Bela, Vryburg, Upington and Musina) projected to experience more than 200 days per year with daily maximum temperatures above 32 °C.

Three stations (Vanwyksvlei, Musina and Upington) are projected to experience 100 days or more annually of daily maximum temperatures above 35 °C in the mid-future under the RCP4.5, which is up from their current annual average frequencies of 59, 78 and 83 days respectively. By the end of the century, Vryburg (44 days annually in the current climate) will join these stations in measuring more than 100 days above 35 °C. Under the RCP8.5 scenario, by the end of the century, a further two stations (Glen College, Bela Bela) are projected to experience these temperatures for more than 100 days on average, which is far above

**Table 3**
Current and projected average number of days per year with temperature above certain critical thresholds. Grey blocks the observation (1976–2005), green blocks indicate the RCP4.5 and yellow RCP 8.5. Days greater than 100 in blue and above 200 in red. The table compares the critical temperature for each station's observed and projected model runs, and thus, it was not fundamentally relevant whether the specific stations passed the K-S test or not. Information on all stations are included and those stations not passing the K-S test are indicated by *.

| Station Name | Obs (1976 – 2005) | | | | RCP4.5 (2036-2065) | | | | RCP4.5 (2066-2095) | | | | RCP8.5 (2036-2065) | | | | RCP8.5 (2066-2095) | | | |
|---|---|---|---|---|---|---|---|---|---|---|---|---|---|---|---|---|---|---|---|---|
| | 32°C | 35°C | 38°C | 46°C | 32°C | 35°C | 38°C | 46°C | 32°C | 35°C | 38°C | 46°C | 32°C | 35°C | 38°C | 46°C | 32°C | 35°C | 38°C | 46°C |
| Cape Agulhas | 0 | 0 | 0 | 0 | 0 | 0 | 0 | 0 | 0 | 0 | 0 | 0 | 0 | 0 | 0 | 0 | 0 | 0 | 0 | 0 |
| Cape Columbine* | 0 | 0 | 0 | 0 | 0 | 0 | 0 | 0 | 1 | 0 | 0 | 0 | 1 | 0 | 0 | 0 | 2 | 0 | 0 | 0 |
| Cape Point | 0 | 0 | 0 | 0 | 1 | 0 | 0 | 0 | 1 | 0 | 0 | 0 | 1 | 0 | 0 | 0 | 3 | 1 | 0 | 0 |
| Cape St. Blaize | 2 | 0 | 0 | 0 | 3 | 1 | 0 | 0 | 4 | 1 | 0 | 0 | 4 | 1 | 0 | 0 | 8 | 2 | 1 | 0 |
| Port Elizabeth* | 6 | 1 | 0 | 0 | 6 | 1 | 0 | 0 | 8 | 1 | 0 | 0 | 8 | 1 | 0 | 0 | 16 | 4 | 1 | 0 |
| Johannesburg | 1 | 0 | 0 | 0 | 13 | 1 | 0 | 0 | 21 | 2 | 0 | 0 | 19 | 2 | 0 | 0 | 64 | 18 | 3 | 0 |
| Cape Town | 7 | 1 | 0 | 0 | 16 | 3 | 0 | 0 | 20 | 4 | 1 | 0 | 20 | 4 | 1 | 0 | 38 | 11 | 2 | 0 |
| Mount Edgecombe* | 10 | 1 | 0 | 0 | 24 | 3 | 0 | 0 | 30 | 4 | 0 | 0 | 30 | 3 | 0 | 0 | 51 | 10 | 1 | 0 |
| Cedara | 11 | 1 | 0 | 0 | 28 | 5 | 0 | 0 | 35 | 7 | 1 | 0 | 34 | 7 | 0 | 0 | 64 | 22 | 4 | 0 |
| Cape St. Lucia | 26 | 4 | 0 | 0 | 54 | 13 | 1 | 0 | 64 | 16 | 2 | 0 | 65 | 16 | 2 | 0 | 110 | 36 | 7 | 0 |
| Polokwane | 19 | 2 | 0 | 0 | 57 | 11 | 1 | 0 | 72 | 18 | 2 | 0 | 71 | 17 | 2 | 0 | 128 | 53 | 12 | 0 |
| Emerald Dale | 33 | 7 | 0 | 0 | 69 | 25 | 5 | 0 | 80 | 32 | 7 | 0 | 80 | 32 | 7 | 0 | 127 | 67 | 25 | 0 |
| Pretoria | 22 | 2 | 0 | 0 | 70 | 16 | 2 | 0 | 91 | 26 | 3 | 0 | 86 | 24 | 3 | 0 | 153 | 72 | 21 | 0 |
| Langgewens | 49 | 20 | 5 | 1 | 76 | 36 | 13 | 0 | 86 | 44 | 17 | 0 | 88 | 45 | 17 | 0 | 121 | 71 | 34 | 1 |
| Beaufort West | 60 | 20 | 2 | 0 | 95 | 44 | 11 | 0 | 107 | 52 | 15 | 0 | 107 | 53 | 16 | 0 | 145 | 86 | 35 | 0 |
| Calvinia | 58 | 18 | 2 | 0 | 97 | 45 | 11 | 0 | 110 | 55 | 16 | 0 | 100 | 51 | 15 | 0 | 151 | 94 | 41 | 0 |
| Vanwyksvlei | 114 | 59 | 16 | 0 | 152 | 101 | 47 | 0 | 163 | 115 | 59 | 0 | 164 | 115 | 59 | 0 | 197 | 154 | 105 | 3 |
| Glen College | 72 | 13 | 0 | 0 | 145 | 52 | 7 | 0 | 170 | 72 | 14 | 0 | 167 | 69 | 13 | 0 | 244 | 152 | 62 | 1 |
| Bela Bela | 82 | 17 | 1 | 0 | 153 | 58 | 11 | 0 | 178 | 78 | 19 | 0 | 174 | 75 | 18 | 0 | 246 | 147 | 59 | 0 |
| Vryburg | 110 | 44 | 9 | 0 | 163 | 93 | 34 | 0 | 180 | 113 | 49 | 0 | 178 | 109 | 46 | 0 | 228 | 165 | 98 | 3 |
| Upington | 140 | 83 | 28 | 0 | 176 | 123 | 65 | 0 | 190 | 137 | 80 | 0 | 190 | 137 | 80 | 0 | 227 | 180 | 127 | 5 |
| Musina | 152 | 78 | 25 | 0 | 204 | 127 | 58 | 0 | 195 | 127 | 63 | 0 | 216 | 140 | 70 | 0 | 234 | 171 | 105 | 3 |

their current rate of occurrence of 13 and 17 days, respectively.

Even more concerning is that some stations (Vanwyksvlei, Upington and Musina) under the RCP8.5 scenario are projected to experience temperatures of greater than 38 °C for more than 100 days per year for the far future, up from a current average of 23 days. Upington currently has no recorded temperatures above 46 °C from 1976 to 2005; however, by the end of the century under the RCP8.5 scenario, this is projected to increase to an average of 5 days a year.

### 3.3. Projected future temperature extremes changes

When looking at the RPs in terms of reaching critical temperatures, under the current climate, four stations (Cape Agulhas, Cape Point, Cape St. Blaize and Cape Columbine) have RPs of greater than a year for 32 °C. However, by the mid-future under RCP4.5 this is the case for only two stations (Cape Agulhas, and Cape Columbine) (Table 4). When considering temperatures of 35 °C and above under RCP8.5, most stations will have RPs of less than 1 year by the end of the century. Considering daily temperatures of 38 °C under RCP4.5 for the mid-(far-) future, 10 (11) stations are projected to experience RPs of less than a year, while under RCP8.5, this will increase to 11 (15) stations. Daily maximum temperatures above 46 °C are extraordinary for South Africa, with 45.3 °C the current high Tmax record for Upington, and 42.5 °C for Musina in the hotter regions of the analysis. What is of concern is that there is a possibility of exceeding this value (46 °C) about every 9 and 6 years for these two stations, respectively, in the far future under RCP4.5. If we consider the RCP8.5, then another four stations (Musina, Vanwyksvlei, Vryburg and Langgewens) are projected to experience return periods of less than 3 years for daily maximum temperature of above 46 °C by the end of the century. Thus, while temperatures above 46 °C are currently not experienced at the stations in this study under RCP8.5 these will occur at least once a year in places such as Vanwyksvlei, Glen College, Bela Bela, Vryburg, Upington and Musina by the end of the century.(see Table 5)

The spatial distribution of change over South Africa for RCP4.5 and RCP8.5 for the mid-and far-futures shows a general increase in 1:10 year extremes, as presented in.

Fig. 3. For RCP4.5 for the mid-future, most stations increase by

**Table 4**
The RPs in years for critical temperatures to be reached under RCP4.5 and RCP8.5 for the period 2036–2065 and 2066–2095. Orange blocks represent RPs of less than a year, while blue block RPs of over 1 000 years. The table compares the critical temperature for each station's projected model runs, and thus, it was not fundamentally relevant whether the specific stations passed the K-S test or not. Information on all stations are included, and those not passing the K-S test are indicated by *.

| Station Name | RCP4.5 (2036-2065) | | | | | RCP4.5 (2066-2095) | | | | | RCP8.5 (2036-2065) | | | | | RCP8.5 (2066-2095) | | | | |
|---|---|---|---|---|---|---|---|---|---|---|---|---|---|---|---|---|---|---|---|---|
| | 32°C | 35°C | 38°C | 46°C | 48°C | 32°C | 35°C | 38°C | 46°C | 48°C | 32°C | 35°C | 38°C | 46°C | 48°C | 32°C | 35°C | 38°C | 46°C | 48°C |
| Cape Agulhas | 34 | 706 | | | | 11 | 144 | | | | 10 | 136 | | | | 4 | 31 | 270 | | |
| Cape Columbine* | 4 | 41 | 427 | | | 2 | 13 | 97 | | | 2 | 15 | 103 | | | | 5 | 35 | | |
| Cape Point | | 7 | 58 | | | | 3 | 20 | | | | 4 | 20 | | | | 1 | 11 | | |
| Johannesburg | | 3 | 53 | | | | 2 | 24 | | | | 2 | 20 | | | | | 2 | 754 | |
| Port Elizabeth* | | 2 | 13 | | | | 1 | 8 | | | | 1 | 8 | | | | | 2 | 294 | 987 |
| Cape St. Blaize | | 1 | 8 | 965 | | | 1 | 5 | 380 | | | 1 | 8 | 606 | | | 1 | 2 | 83 | 206 |
| Mount Edgecombe* | | | 7 | | | | | 4 | | | | | 6 | | | | | 1 | | |
| Cedara | | | 7 | | | | | 3 | | | | | 4 | | | | | 1 | 343 | |
| Polokwane | | | 3 | | | | | 1 | | | | | 1 | | | | | | 226 | |
| Cape Town | | | 5 | | | | | 3 | | | | | 2 | | | | | 1 | 270 | |
| Pretoria | | | 2 | | | | | 1 | | | | | 1 | 750 | | | | | 48 | 211 |
| Cape St. Lucia | | | 1 | | | | | | 513 | | | | | 581 | | | | | 161 | 857 |
| Glen College | | | 1 | 287 | | | | | 74 | 307 | | | | 95 | 399 | | | | 4 | 12 |
| Emerald Dale | | | | 522 | | | | | 250 | | | | | 134 | 714 | | | | 10 | 40 |
| Bela Bela | | | | | | | | | 550 | | | | | 246 | | | | | 16 | 100 |
| Beaufort West | | | | | | | | | 520 | | | | | 378 | | | | | 38 | 383 |
| Calvinia | | | | 298 | | | | | 213 | | | | | 139 | | | | | 14 | 91 |
| Vanwyksvlei | | | | 100 | | | | | 30 | 292 | | | | 22 | 154 | | | | 2 | 13 |
| Vryburg | | | | 44 | 248 | | | | 19 | 111 | | | | 20 | 97 | | | | 2 | 10 |
| Langgewens | | | | 32 | 187 | | | | 11 | 52 | | | | 10 | 43 | | | | 3 | 11 |
| Upington | | | | 22 | 177 | | | | 9 | 71 | | | | 8 | 57 | | | | 1 | 7 |
| Musina | | | | 9 | 60 | | | | 6 | 40 | | | | 5 | 33 | | | | | 5 |

**Table 5**
List of stations with their current return period quantile values (C°) for 10-,50- and 100-years (green columns). This is followed by the projected RPs for the current return period quantile values under the RCP4.5 and RCP8.5 for the two study periods of mid- (2036–2065) (blue columns) and far-future (2066–2095) (orange columns). (e.g. The current 1 in 10-year value for Cape Agulhas is 30.1 °C, the value of which is projected to have an RP of 3.5 years under the RCP 4.5 scenario in the 2036–2065 period).

| Station name | Current return period quantile values (1976 to 2005) | | | Projected return periods of current return period quantile values | | | | | | | | | | | |
|---|---|---|---|---|---|---|---|---|---|---|---|---|---|---|---|
| Return period quantile values | 10yr | 50yr | 100yr | RCP4.5 (2036-2065) | | | RCP4.5 (2066-2095) | | | RCP8.5 (2036-2065) | | | RCP8.5 (2066-2095) | | |
| Cape Agulhas | 30.1 | 31.5 | 32.1 | 3.5 | 14.7 | 27.3 | 2.1 | 7.0 | 11.8 | 2.0 | 6.7 | 11.4 | 0.9 | 2.5 | 3.9 |
| Cape Point | 32.8 | 35.0 | 35.9 | 1.5 | 6.9 | 13.3 | 0.7 | 2.9 | 5.2 | 1.2 | 3.8 | 5.2 | 0.2 | 0.6 | 0.8 |
| Cape St. Blaize | 35.2 | 37.4 | 38.4 | 1.6 | 5.9 | 10.4 | 1.1 | 3.7 | 6.2 | 1.6 | 5.4 | 9.2 | 0.6 | 1.7 | 2.5 |
| Cape Town | 37.2 | 39.0 | 39.8 | 2.5 | 15.2 | 32.8 | 1.4 | 5.8 | 10.6 | 1.2 | 4.7 | 8.7 | 0.4 | 1.6 | 2.8 |
| Cape St. Lucia | 38.6 | 40.3 | 41.0 | 1.8 | 8.0 | 15.3 | 1.3 | 5.1 | 9.4 | 1.4 | 5.7 | 10.5 | 0.3 | 1.4 | 2.5 |
| Langgewens | 43.1 | 45.0 | 45.9 | 2.3 | 13.2 | 27.9 | 1.1 | 4.8 | 8.9 | 1.1 | 4.9 | 9.9 | 0.3 | 1.2 | 2.3 |
| Beaufort West | 40.1 | 41.3 | 41.8 | 0.6 | 2.8 | 5.4 | 0.3 | 1.5 | 2.8 | 0.3 | 1.5 | 2.8 | 0.0 | 0.2 | 0.3 |
| Calvinia | 40.3 | 41.7 | 42.3 | 0.9 | 3.7 | 6.9 | 0.4 | 1.8 | 3.6 | 0.5 | 1.9 | 3.5 | 0.1 | 0.3 | 0.5 |
| Vanwyksvlei | 41.8 | 43.0 | 43.5 | 0.7 | 2.9 | 5.4 | 0.2 | 0.9 | 1.7 | 0.3 | 1.1 | 1.9 | 0.0 | 0.1 | 0.2 |
| Emerald Dale | 38.8 | 40.2 | 40.9 | 0.7 | 2.7 | 4.8 | 0.3 | 1.3 | 2.3 | 0.3 | 1.1 | 1.9 | 0.1 | 0.2 | 0.3 |
| Cedara | 36.0 | 37.3 | 37.8 | 0.8 | 3.1 | 5.5 | 0.4 | 1.6 | 2.8 | 0.5 | 1.8 | 3.3 | 0.1 | 0.3 | 0.5 |
| Glen College | 38.7 | 40.2 | 40.8 | 0.9 | 2.9 | 4.8 | 0.4 | 1.2 | 1.9 | 0.5 | 1.5 | 2.4 | 0.1 | 0.3 | 0.4 |
| Upington | 42.8 | 44.0 | 44.5 | 0.7 | 2.7 | 4.8 | 0.3 | 1.1 | 2.0 | 0.4 | 1.2 | 2.0 | 0.0 | 0.1 | 0.2 |
| Vryburg | 41.5 | 43.2 | 43.9 | 0.9 | 3.8 | 7.1 | 0.4 | 1.6 | 3.1 | 0.6 | 2.2 | 3.8 | 0.1 | 0.2 | 0.4 |
| Johannesburg | 33.5 | 35.1 | 35.8 | 0.8 | 3.7 | 7.1 | 0.4 | 1.7 | 3.2 | 0.5 | 1.9 | 3.4 | 0.1 | 0.2 | 0.3 |
| Pretoria | 37.0 | 38.7 | 39.4 | 0.9 | 4.0 | 7.7 | 0.4 | 1.9 | 3.6 | 0.6 | 2.2 | 3.9 | 0.1 | 0.2 | 0.4 |
| Bela Bela | 39.4 | 40.8 | 41.5 | 0.6 | 3.3 | 6.9 | 0.3 | 1.4 | 3.0 | 0.4 | 1.6 | 3.0 | 0.0 | 0.1 | 0.2 |
| Polokwane | 37.0 | 38.6 | 39.3 | 0.9 | 4.4 | 8.6 | 0.5 | 2.3 | 4.4 | 0.6 | 2.4 | 4.5 | 0.1 | 0.3 | 0.5 |
| Musina | 43.6 | 45.2 | 45.8 | 1.0 | 4.2 | 7.8 | 0.5 | 2.4 | 4.6 | 0.6 | 2.5 | 4.5 | 0.1 | 0.3 | 0.6 |

2 °C–3 °C compared with the current climate. This warming is set to increase by a further 1 °C in the far future for this RCP. It is predicted that Glen College (central Free State) will have the highest increase of 4.2 °C by the end of the century. Under the RCP8.5 scenario, the return period quantile values for the mid-future showed most stations are projected to experience an increase in 1 in10 year extremes of 2 °C–3.8 °C. Thus, warming for the mid-future for RCP8.5 is similar to the warming projected for the far-future under the RCP4.5 scenario, indicating that the warming is likely to occur at an increased rate under RCP8.5 compared to RCP4.5. By the end of the 21st century, under the RCP8.5 scenario, most stations are projected to experience return period quantile value changes of greater than 4 °C with places such as Emerald Dale and Glen College by as much as 7.2 °C and 8.9 °C respectively. The averages of return period quantile values for the near-future (far-future) under the RCP4.5 are 40.6 °C (41.5 °C); however, if RCP8.5 materializes, the average will increase to 43.8 °C by the end of the century. The models generally underestimate the change compared to the observational period, meaning that the projected return period quantile values will possibly be even higher.

Fig. 4 presents the average increase in the 50-year return period quantile values, reflecting a similar spatial pattern as the results shown in Fig. 3. In the mid-future for RCP4.5, the increase is predicted to be, on average, around 2.4 °C increasing by about another 1.0 °C in the far-future period. The return period quantile values are, on average, projected to be 42.4 °C (43.3 °C) for the mid-future (far-future) under RCP4.5. Under RCP8.5, the mid-future change is projected to be between 1.8 °C and 3.8 °C, increasing in the far future to above 4.0 °C for all stations. Emerald Dale and Glen College are projected to experience the greatest change of 8.0 °C and 10.8 °C, respectively, by the end of the century. Under RCP8.5, these mid-future (far-future) return period quantile values are projected to increase to an average of 43.5 °C (46 °C) respectively. Once again, the models generally underestimate the change compared to the observational period, which means that the projected return period quantile values could be even higher. This is especially true for stations like Cape Agulhas, Beaufort West, Cape Point and Bela, Bela which showed more than 3 °C underestimation in terms of the models representing the 50-year return period quantile values compared to the observed return period quantile values.

### 3.4. *Quantile values for specific periods*

The study then investigated the projected RPs for the 10-, 50- and 100-year current return period quantiles values given the alpha and beta values derived from the RCP4.5 and RCP8.5 for the mid-and far-futures (equation (4)) (Table). The current 10-year return period quantile values are projected to occur at least once in a typical year at most places in the

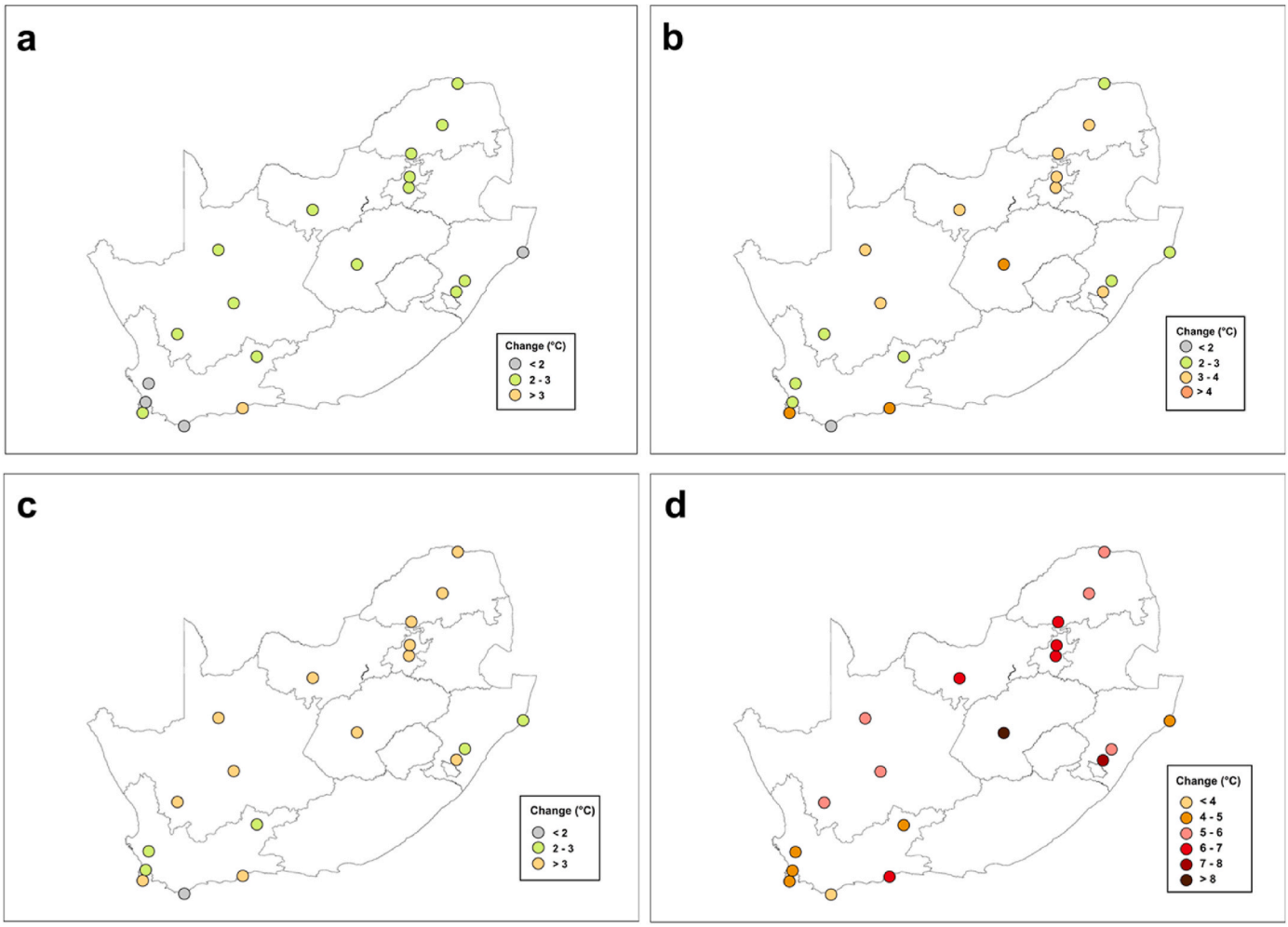


**Fig. 3.** The change in estimated 10-year return period quantile values for RCP4.5 for mid-future (2036–2065) (a) and for far-future (2066–2095) (b), and RCP8.5 scenarios 2036–2065 (c) and 2066–2095 (d). Port Elizabeth, Cape Columbine and Mount Edgecombe did not have any of their models pass the K-S test at the 5% level after bias correction, and thus, the RPs were not calculated.

interior in the RCP4.5 scenario for the mid-future, while coastal stations are projected to have RPs of between 1.5 and 3.5 years.

In terms of the current 50-year return period quantile values for the RCP4.5, interior stations (coastal stations) are projected to have RPs of 3–4 (6–15) years for the mid-future, while for the far future, this is projected to decrease to 1 to 2 (3–7) years. For the RCP8.5, the current 50-year return period quantile values are projected to occur more often with most interior stations projected to have return period quantile values shorter than a year by the end of the century. For coastal stations, the RPs are expected to decrease to three years or shorter.

When considering current return period quantile values of 100 years, these values would have, for most interior stations for mid-future (far-future) for the RCP4.5, RPs of 5–9 years (2–5 years), while coastal stations are projected for RPs of 13–33 years (5–12 years). When considering the RCP8.5 scenario, most interior stations will have RPs of 1 year or less by the end of the century, with coastal stations having slightly longer RPs of up to 4 years.

## 4. Discussion and conclusions

This study analysed the return periods of high daily temperature extremes over South Africa, focusing on projections of these conditions under the RCP 4.5 and 8.5 scenarios for two future periods (2036–2065 and 2066–2095). A verified subset of CORDEX model data was used, and the period of 1976–2005 was selected for comparison between observed and the model temperatures at 22 locations over South Africa. Bias corrections, which preserved the long-term trend with respect to the monthly mean values, were conducted to provide confidence in the projected absolute values of the temperatures. This method is advocated for by Casanueva et al. (2020) because it maintains the original raw climate change signal while alleviating biases. After the bias correction, the models showed an underestimation of the return period quantile values compared to the observational return period quantile values. This underestimation of maximum temperature when using CORDEX data has also been found over southwest Ethiopia (Demissie and Sime, 2021), Malawi (Warnatzsch and Reay, 2019), Africa (Soares et al., 2019), Australasia (Evans et al., 2021) and Australia (Di Virgilio et al., 2019). Thus, it is suggested that the projected return period quantile values in this study could be higher, and therefore, the results should be used with caution – for example minimum estimates. It should also be noted that uncertainty in the return period quantile values normally increase for longer periods.

The statistical analysis of the daily temperature extremes in this study found that return period quantile values are likely to increase under both RCPs in the mid- (2036–2065) and far-future (2066–2095) periods. The highest increase in return period quantile values is set to occur towards the end of the century under a high emission scenario compared to the mid-future or under a RCP4.5 scenario. When considering extreme temperature changes, the 50-year return period quantile values under the RCP4.5 for mid- (far-) future for most stations are

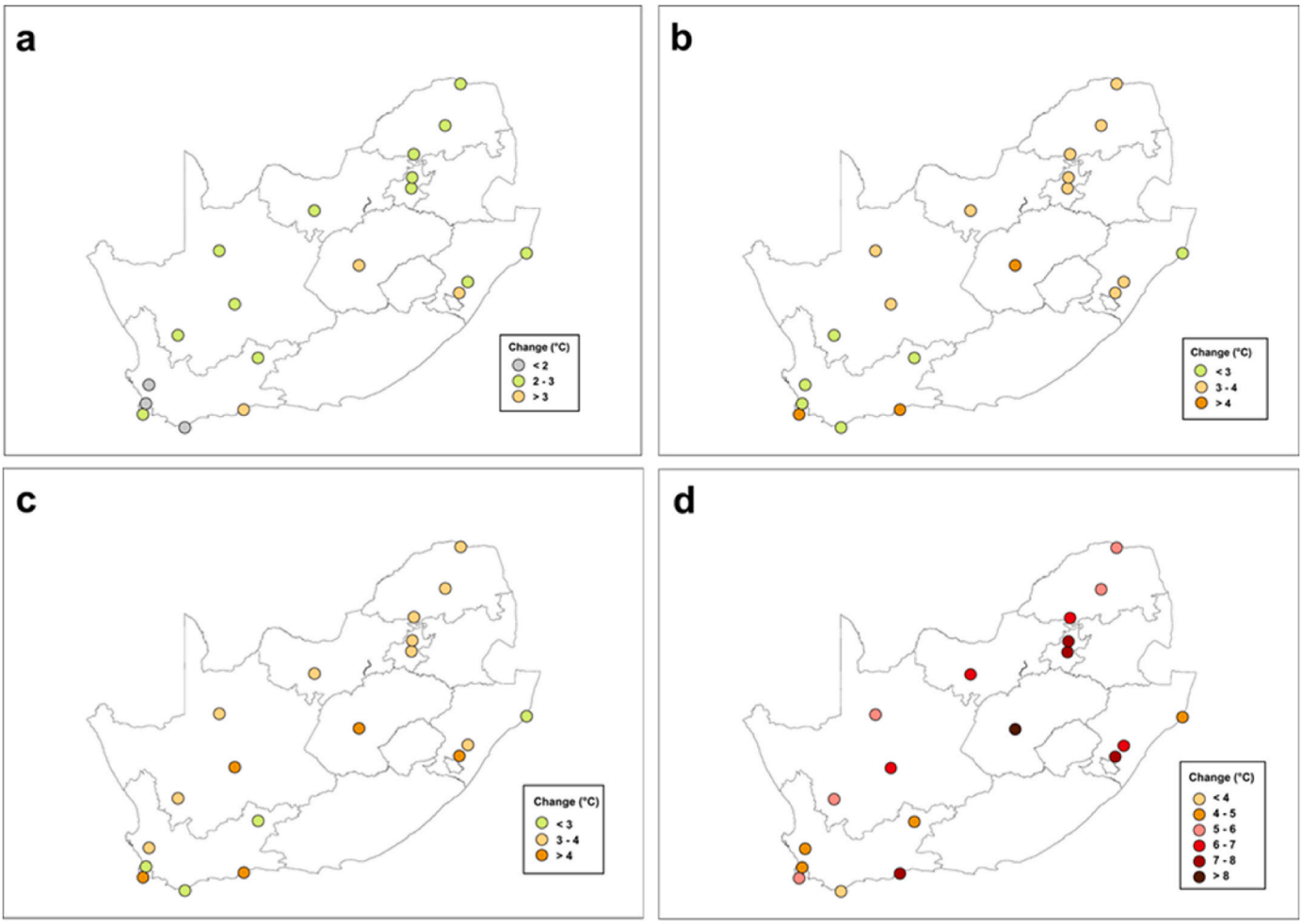


**Fig. 4.** The change in estimated 50 year return period quantile values for RCP4.5 for 2036–2065 (a) 2066–2095 (b), and RCP8.5 scenarios 2036–2065 (c) and 2066–2095 (d). Port Elizabeth, Cape Columbine and Mount Edgecombe did not have any of their models pass the K-S test at the 5% level after bias correction and thus, RPs were not calculated.

projected to increase by 2 °C–3 °C (3 °C–4 °C) compared with the period of 1976–2005. The 50-year return period quantile values for interior stations, under the RCP8.5 scenario, are projected to have temperature increases of greater than 5 °C compared to the current climate by the end of the century. Interior stations showed higher return period quantile values for all scenarios and periods when compared to most coastal stations, indicating the possible moderating effect of the ocean on temperatures. These findings are very similar to those of Archer et al. (2018) and Almazroui et al. (2020), who also found similar projected increases in temperatures with higher projected increases over the interior compared to coastal areas. This study used one CORDEX regional climate model and thus the results are 'model dependent'. Future studies might like to consider additional observation-verified regional models and updates thereof, to investigate if they provide similar findings and help to better describe the uncertainties associated with the projections.

Despite the fact that in this study, these models possibly underestimated the probability of extreme temperatures, there is still have the potential for extremes to be exacerbated, due to the projected increase in dry spells (Haensler et al., 2011). This will contribute to the frequency and intensity of heat wave events over South Africa (Engelbrecht et al., 2015; Dosio, 2017; Mbokodo et al., 2023) and increase the risk of high fire danger days (Singo et al., 2023).

High temperatures are also of major concern for human, animal and crop health. More than half the stations in the study are set to record more than 100 days of temperature above 32 °C annually by the end of the century under the RCP8.5. Six of these stations, all in the country's interior, are projected to experience more than 200 days of temperatures above 32 °C annually. These types of temperatures can cause adverse respiratory and cardiovascular effects and are of concern among the elderly, those in poor health and/or those with limited or no access to medical facilities (Garland et al., 2015; Bühler et al., 2022). In terms of agriculture, crop seedling diseases increase in temperatures above 32 °C when the soil is saturated (Rosenzweig et al., 2001), and dairy cows suffer severe heat stress in these temperatures (Bohmanova et al., 2007). There is thus a need for awareness to be created to target vulnerable communities and industries regarding the dangers of the predicted changes in daily temperatures, as well as providing strategies to prevent loss of life and livelihoods.

In terms of higher temperatures above 35 °C (38 °C), six (three) of the stations in the study are projected to exceed these temperatures more than 100 days annually by the end of the century under the RCP8.5. These high temperatures are of major concern from a health perspective as they have the potential to cause heat exhaustion, leading to heat stroke, especially if one is engaged in physical activities such as manual labour or one lacks access to adequate air conditioning (Garland et al., 2015; Fotso-Nguemo et al., 2023).

These projected extreme temperatures may be exacerbated by the urban heat island effect, and thus, mitigation measures in terms of how we construct our houses and cities needs to be timeously reviewed (Luber and McGeehin, 2008). Rainfed agricultural systems are vulnerable to changes in climate (Serdeczny et al., 2017), especially high

temperatures (Zhu and Troy, 2018). These high temperatures can cause various degrees of damage depending on the duration of the temperatures and the developmental stage of the crop (Rosenzweig et al., 2001). This, coupled with too much or too little rainfall, can make matters worse (Rosenzweig et al., 2001). The behaviour of pollinators can also be affected where, for example, honey bees spend more time collecting water to cool the hive than delivering crop pollination services (Rader et al., 2013). There is thus a need to consider the vulnerability of the types of crops grown and those who grow crops and or keep livestock, especially in the case of subsistence farming (Thornton et al., 2021). Plans need to be implemented to assist these farmers, for example with the provision of shade and necessary water for their crops and animals. In a study in KwaZulu-Natal by Hlahla and Hill (2018), it was found that local communities felt they lacked knowledge about climate change and believed they could do nothing to deal with the impacts, thus education on farming adaptions will become increasingly important as the climate changes.

It is suggested that relatively more consideration be given to changes in extremes rather than just changes in the mean. This is because small, as illustrated by the study, changes in mean annual temperature can lead to significant changes in the probability of hot extremes. Therefore, industries affected by changes in climate will be advised not to base their assessments of future climate scenarios solely on changes in mean temperature. If they do this, they could be considering lower estimates of change rather than if they had considered changes related to extreme daily temperatures. By way of example, when looking at adaptation strategies to effectively reduce the impact of heat stress on domesticated livestock, if decisions are based solely on projected increases in mean temperature rather than changes in extreme temperatures, these interventions may not necessarily be adequate in providing the anticipated adequate protection for reducing the heat stress, and thus additional investment may be needed at a later stage (which were not originally planned for).

The results of this study suggest that South Africa is likely to experience a strong increase in the intensity, duration, and frequency of hot extremes in the future, with a caveat that the projected quantities may not be considered optimal until the full set of CORDEX model outputs have been similarly analysed. In essence, despite the fact that the models were used in earlier studies, and the fact that they passed evaluation criteria, they were not evaluated in a way which would allow them to be considered better-performing than the remainder of the CORDEX ensemble, and consequently - represent future changes better than the entire ensemble, with consequences to the uncertainty of results. However, while the quantification is not optimal, it can be assumed that extreme temperatures are set to increase at a faster rate than the mean temperature increase, with therefore an urgent need for South Africa to heed the call made by Ziervogel et al. (2022) to become climate resilient and look for ways to develop “Climate Resilient Development Pathways”. It also needs to do all it can to advocate for a global reduction of greenhouse gas emissions, as high concentrations of these gases in the atmosphere will lead to disproportionate increases in localized hot extremes, to what the projected general warming suggests.

## CRediT authorship contribution statement

**Charlotte M. McBride:** Writing – review & editing, Writing – original draft, Visualization, Validation, Project administration, Methodology, Investigation, Funding acquisition, Formal analysis, Data curation, Conceptualization. **Andries C. Kruger:** Writing – review & editing, Validation, Supervision, Methodology, Conceptualization. **Charmaine Johnston:** Writing – review & editing, Software. **Liesl Dyson:** Writing – review & editing.

## Declaration of competing interest

The authors declare that they have no known competing financial interests or personal relationships that could have appeared to influence the work reported in this paper.

## Acknowledgements

We thank the Coordinated Regional Climate Downscaling Experiment (CORDEX) for the availability of model data for this study.

## Data availability

Data will be made available on request.

## References

Ahmadalipour, A., Rana, A., Moradkhani, H., Sharma, A., 2017. Multi-criteria evaluation of CMIP5 GCMs for climate change impact analysis. Theor. Appl. Climatol. 128 (1–2), 71–87. https://doi.org/10.1007/s00704-015-1695-4.

Alexander, L.V., Arblaster, J.M., 2009. Assessing trends in observed and modelled climate extremes over Australia in relation to future projections. Int. J. Climatol. 29 (3), 417–435. https://doi.org/10.1002/joc.1730.

Alexander, L.V., Arblaster, J.M., 2017. Historical and projected trends in temperature and precipitation extremes in Australia in observations and CMIP5. Weather Clim. Extrem. 15, 34–56. https://doi.org/10.1016/j.wace.2017.02.001.

Almazroui, M., Saeed, F., Saeed, S., Nazrul Islam, M., Ismail, M., Klutse, N.A.B., Siddiqui, M.H., 2020. Projected change in temperature and precipitation over Africa from CMIP6. Earth Systems Environ. 4 (3), 455–475. https://doi.org/10.1007/s41748-020-00161-x.

Almazroui, M., Saeed, F., Saeed, S., Ismail, M., Ehsan, M.A., Islam, M.N., Abid, M.A., O'Brien, E., Kamil, S., Rashid, I.U., Nadeem, I., 2021. Projected changes in climate extremes using CMIP6 simulations over SREX regions. Earth Systems Environ. 5 (3), 481–497. https://doi.org/10.1007/s41748-021-00250-5.

Anyamba, A., Small, J.L., Britch, S.C., Tucker, C.J., Pak, E.W., Reynolds, C.A., Crutchfield, J., Linthicum, K.J., 2014. Recent weather extremes and impacts on agricultural production and vector-borne disease outbreak patterns. PLoS One 9 (3), e92538. https://doi.org/10.1371/journal.pone.0092538.

Archer, E., Engelbrecht, F., Hänsler, A., Landman, W., Tadross, M., Helmschrot, J., 2018. Seasonal prediction and regional climate projections for southern Africa. Biodiversity Ecol. 6, 14–21. https://doi.org/10.7809/b-e.00296.

Technical summary. In: Arias, P.A., Bellouin, N., Coppola, E., Jones, R.G., Krinner, G., Marotzke, J., Naik, V., Palmer, M.D., Plattner, G.-K., Rogelj, J., Rojas, M., Sillmann, J., Storelvmo, T., Thorne, P.W., Trewin, B., Achuta Rao, K., Adhikary, B., Allan, R.P., Armour, K., Bala, G., Barimalala, R., Berger, S., Canadell, J.G., Cassou, C., Cherchi, A., Collins, W., Collins, W.D., Connors, S.L., Corti, S., Cruz, F., Dentener, F.J., Dereczynski, C., Di Luca, A., Diongue Niang, A., Doblas-Reyes, F.J., Dosio, A., Douville, H., Engelbrecht, F., Eyring, V., Fischer, E., Forster, P., Fox-Kemper, B., Fuglestvedt, J.S., Fyfe, J.C., Gillett, N.P., Goldfarb, L., Gorodetskaya, I., Gutierrez, J.M., Hamdi, Hawkins, E., Hewitt, H.T., Hope, P., Islam, A.S., Jones, C., Kaufman, D.S., Kopp, R.E., Kosaka, Y., Kossin, J., Krakovska, S., Lee, J.-Y., Li, J., Mauritsen, T., Maycock, K., Meinshausen, M., Min, S.-K., Monteiro, P.M.S., Ngo-Duc, T., Otto, F., Pinto, I., Pirani, A., Raghavan, K., Ranasinghe, R., Ruane, A.C., Ruiz, L., Sallée, J.-B., Samset, B.H., Sathyendranath, S., Seneviratne, S.I., Sörensson, A.A., Szopa, S., Takayabu, I., Tréguier, A.-M., Van den Hurk, B., Vautard, R., Von Schuckmann, K., Zaehle, S., Zhang, X., Zickfeld, K. (Eds.), 2021. Climate Change 2021: the Physical Science Basis. Cambridge University Press, Cambridge, United Kingdom and New York, NY, USA.

Arora, V.K., Scinocca, J.F., Boer, G.J., Christian, J.R., Denman, K.L., Flato, G.M., Kharin, V.V., Lee, W.G., Merryfield, W.J., 2011. Carbon emission limits required to satisfy future representative concentration pathways of greenhouse gases. Geophys. Res. Lett. 38 (5), n/a. https://doi.org/10.1029/2010gl046270 n/a.

Asefi-Najafabady, S., Vandecar, K.L., Seimon, A., Lawrence, P., Lawrence, D., 2018. Climate change, population, and poverty: vulnerability and exposure to heat stress in countries bordering the Great Lakes of Africa. Clim. Change 148 (4), 561–573. https://doi.org/10.1007/s10584-018-2211-5.

Blackshaw, J., Blackshaw, A., 1994. Heat stress in cattle and the effect of shade on production and behaviour: a review. Aust. J. Exp. Agric. 34 (2), 285. https://doi.org/10.1071/ea9940285.

Bohmanova, J., Misztal, I., Cole, J.B., 2007. Temperature-humidity indices as indicators of milk production losses due to heat stress. J. Dairy Sci. 90 (4), 1947–1956. https://doi.org/10.3168/jds.2006-513.

Botai, C.M., Botai, J.O., Zwane, N.N., Hayombe, P., Wamiti, E.K., Makgoale, T., Murambadoro, M.D., Adeola, A.M., Ncongwane, K.P., De Wit, J.P., Mengistu, M.G., Tazvinga, H., 2020. Hydroclimatic extremes in the limpopo river basin, South Africa, under changing climate. Water 12 (12), 3299. https://doi.org/10.3390/w12123299.

Bröde, P., Fiala, D., Błażejczyk, K., Holmér, I., Jendritzky, G., Kampmann, B., Tinz, B., Havenith, G., 2012. Deriving the operational procedure for the universal thermal climate index (UTCI). Int. J. Biometeorol. 56 (3), 481–494. https://doi.org/10.1007/s00484-011-0454-1.

Bühler, J.L., Shrikhande, S., Kapwata, T., Cissé, G., Liang, Y., Pedder, H., Kwiatkowski, M., Kunene, Z., Mathee, A., Peer, N., Wright, C.Y., 2022. The association between apparent temperature and hospital admissions for cardiovascular disease in limpopo province, South Africa. Int. J. Environ. Res. Publ. Health 20 (1), 116. https://doi.org/10.3390/ijerph20010116.

Burke, M.B., Miguel, E., Satyanath, S., Dykema, J.A., Lobell, D.B., 2009. Warming increases the risk of civil war in Africa. Proc. Natl. Acad. Sci. USA 106 (49), 20670–20674. https://doi.org/10.1073/pnas.0907998106.

Casanueva, A., Herrera, S., Iturbide, M., Lange, S., Jury, M., Dosio, A., Maraun, D., Gutiérrez, J.M., 2020. Testing bias adjustment methods for regional climate change applications under observational uncertainty and resolution mismatch. Atmos. Sci. Lett. 21 (7). https://doi.org/10.1002/asl.978.

Chapman, S., Birch, C.E., Marsham, J.H., Part, C., Hajat, S., Chersich, M.F., Ebi, K.L., Luchters, S., Nakstad, B., Kovats, S., 2022. Past and projected climate change impacts on heat-related child mortality in Africa. Environ. Res. Lett. 17 (7), 074028. https://doi.org/10.1088/1748-9326/ac7ac5.

Chersich, M., Wright, C., Venter, F., Rees, H., Scorgie, F., Erasmus, B., 2018. Impacts of climate change on health and wellbeing in South Africa. Int. J. Environ. Res. Publ. Health 15 (9), 1884–1898. https://doi.org/10.3390/ijerph15091884.

Collins, J.M., 2011. Temperature variability over Africa. J. Clim. 24 (14), 3649–3666. https://doi.org/10.1175/2011JCLI3753.1.

Dell, M., Jones, B.F., Olken, B.A., 2012. Temperature shocks and economic growth: evidence from the last half century. Am. Econ. J. Macroecon. 4 (3), 66–95. https://doi.org/10.1257/mac.4.3.66.

Demissie, T.A., Sime, C.H., 2021. Assessment of the performance of CORDEX regional climate models in simulating rainfall and air temperature over southwest Ethiopia. Heliyon 7 (8), e07791. https://doi.org/10.1016/j.heliyon.2021.e07791.

Di Virgilio, G., Evans, J.P., Di Luca, A., Olson, R., Argüeso, D., Kala, J., Andrys, J., Hoffmann, P., Katzfey, J.J., Rockel, B., 2019. Evaluating reanalysis-driven CORDEX regional climate models over Australia: model performance and errors. Clim. Dyn. 53 (5–6), 2985–3005. https://doi.org/10.1007/s00382-019-04672-w.

Dosio, A., 2017. Projection of temperature and heat waves for Africa with an ensemble of CORDEX regional climate models. Clim. Dyn. 49 (1–2), 493–519. https://doi.org/10.1007/s00382-016-3355-5.

Dunne, J.P., John, J.G., Adcroft, A.J., Griffies, S.M., Hallberg, R.W., Shevliakova, E., Stouffer, R.J., Cooke, W., Dunne, K.A., Harrison, M.J., Krasting, J.P., Malyshev, S.L., Milly, P.C.D., Phillipps, P.J., Sentman, L.T., Samuels, B.L., Spelman, M.J., Winton, M., Wittenberg, A.T., Zadeh, N., 2012. GFDL's ESM2 global coupled climate–carbon earth system models. Part I: physical formulation and baseline simulation characteristics. J. Clim. 25 (19), 6646–6665. https://doi.org/10.1175/jcli-d-11-00560.1.

Endris, H.S., Omondi, P., Jain, S., Lennard, C., Hewitson, B., Chang'A, L., Awange, J.L., Dosio, A., Ketiem, P., Nikulin, G., Panitz, H.-J., Büchner, M., Stordal, F., Tazalika, L., 2013. Assessment of the performance of CORDEX regional climate models in simulating east african rainfall. J. Clim. 26 (21), 8453–8475. https://doi.org/10.1175/jcli-d-12-00708.1.

Engelbrecht, F., Adegoke, J., Bopape, M.-J., Naidoo, M., Garland, R., Thatcher, M., McGregor, J., Katzfey, J., Werner, M., Ichoku, C., Gatebe, C., 2015. Projections of rapidly rising surface temperatures over Africa under low mitigation. Environ. Res. Lett. 10, 10.1088/1748-9326/10.

Evans, J.P., Di Virgilio, G., Hirsch, A.L., Hoffmann, P., Remedio, A.R., Ji, F., Rockel, B., Coppola, E., 2021. The CORDEX-Australasia ensemble: evaluation and future projections. Clim. Dyn. 57 (5–6), 1385–1401, 10.1007/s00382-020-05459-0.

Fischer, E.M., Knutti, R., 2014. Detection of spatially aggregated changes in temperature and precipitation extremes. Geophys. Res. Lett. 41 (2), 547–554. https://doi.org/10.1002/2013gl058499.

Fotso-Nguemo, T.C., Weber, T., Diedhiou, A., Chouto, S., Vondou, D.A., Rechid, D., Jacob, D., 2023. Projected impact of increased global warming on heat stress and exposed population over Africa. Earths Future 11 (1). https://doi.org/10.1029/2022ef003268.

Frías, M.D., Mínguez, R., Gutiérrez, J.M., Méndez, F.J., 2012. Future regional projections of extreme temperatures in Europe: a nonstationary seasonal approach. Clim. Change 113 (2), 371–392. https://doi.org/10.1007/s10584-011-0351-y.

Garland, R., Matooane, M., Engelbrecht, F., Bopape, M.-J., Landman, W., Naidoo, M., Merwe, J., Wright, C., 2015. Regional projections of extreme apparent temperature days in Africa and the related potential risk to human health. Int. J. Environ. Res. Publ. Health 12 (10), 12577–12604. https://doi.org/10.3390/ijerph121012577.

Giorgi, F., 2019. Thirty years of regional climate modeling: where are we and where are we going next? J. Geophys. Res. Atmos. https://doi.org/10.1029/2018jd030094.

Haensler, A., Hagemann, S., Jacob, D., 2011. The role of the simulation setup in a long-term high-resolution climate change projection for the southern African region. Theor. Appl. Climatol. 106 (1–2), 153–169. https://doi.org/10.1007/s00704-011-0420-1.

Hegerl, G.C., Zwiers, F.W., Stott, P.A., Kharin, V.V., 2004. Detectability of anthropogenic changes in annual temperature and precipitation extremes. J. Clim. 17 (19), 3683–3700. https://doi.org/10.1175/1520-0442(2004)017<3683:doacia>2.0.co;2.

Hempel, S., Frieler, K., Warszawski, L., Schewe, J., Piontek, F., 2013. A trend-preserving bias correction – the ISI-MIP approach. Earth Syst. Dynamics 4 (2), 219–236. https://doi.org/10.5194/esd-4-219-2013.

Hirabayashi, Y., Mahendran, R., Koirala, S., Konoshima, L., Yamazaki, D., Watanabe, S., Kim, H., Kanae, S., 2013. Global flood risk under climate change. Nat. Clim. Change 3 (9), 816–821. https://doi.org/10.1038/nclimate1911.

Hlahla, S., Hill, T.R., 2018. Responses to climate variability in urban poor communities in pietermaritzburg, KwaZulu-natal, South Africa. Sage Open 1–16. https://doi.org/10.1177/2158244018800914.

Hosking, J.R.M., 1990. L-moments: analysis and estimation of distributions using linear combinations of order statistics. J. Roy. Stat. Soc. B 52 (1), 105–124. https://doi.org/10.1111/j.2517-6161.1990.tb01775.x.

Hourdin, F., Foujols, M.-A., Codron, F., Guemas, V., Dufresne, J.-L., Bony, S., Denvil, S., Guez, L., Lott, F., Ghattas, J., Braconnot, P., Marti, O., Meurdesoif, Y., Bopp, L., 2013. Impact of the LMDZ atmospheric grid configuration on the climate and sensitivity of the IPSL-CM5A coupled model. Clim. Dyn. 40 (9–10), 2167–2192. https://doi.org/10.1007/s00382-012-1411-3.

Ilyina, T., Six, K.D., Segschneider, J., Maier-Reimer, E., Li, H., Núñez-Riboni, I., 2013. Global ocean biogeochemistry model HAMOCC: model architecture and performance as component of the MPI-Earth system model in different CMIP5 experimental realizations. J. Adv. Model. Earth Syst. 5 (2), 287–315. https://doi.org/10.1029/2012ms000178.

IPCC, 2013. 'Long-term climate change: projections, commitments and irreversibility. In: Stocker, T.F., Qin, D., Plattner, G.-K., Tignor, Allen, S.K., Boschung, J., Nauels, A., Xia, Y., Bex, V., Midgley, P.M. (Eds.), Climate Change 2013: the Physical Science Basis'. Cambridge University Press, United Kingdom and New York, NY, USA. Contribution of Working Group I to the Fifth Assessment Report of the Intergovernmental Panel on Climate Change Cambridge.

Iturbide, M., Casanueva, A., Bedia, J., Herrera, S., Milovac, J., Gutiérrez, J.M., 2022. On the need of bias adjustment for more plausible climate change projections of extreme heat. Atmos. Sci. Lett. 23 (2). https://doi.org/10.1002/asl.1072.

Jury, M.R., 1985. Mesoscale variations in summer winds over the Cape columbine — st helena bay region, South Africa. S. Afr. J. Mar. Sci. 3 (1), 77–88. https://doi.org/10.2989/025776185784461162.

Katz, R.W., Brown, B.G., 1992. Extreme events in a changing climate: variability is more important than averages. Clim. Change 21 (3), 289–302. https://doi.org/10.1007/bf00139728.

Kharin, V.V., Zwiers, F.W., 2005. Estimating extremes in transient climate change simulations. J. Clim. 18 (8), 1156–1173. https://doi.org/10.1175/jcli3320.1.

Kharin, V.V., Zwiers, F.W., Zhang, X., 2005. Intercomparison of near-surface temperature and precipitation extremes in AMIP-2 simulations, reanalyses, and observations. J. Clim. 18 (24), 5201–5223. https://doi.org/10.1175/jcli3597.1.

Kharin, V.V., Zwiers, F.W., Zhang, X., Hegerl, G.C., 2007. Changes in temperature and precipitation extremes in the IPCC ensemble of global coupled model simulations. J. Clim. 20 (8), 1419–1444. https://doi.org/10.1175/jcli4066.1.

Kharin, V.V., Zwiers, F.W., Zhang, X., Wehner, M., 2013. Changes in temperature and precipitation extremes in the CMIP5 ensemble. Clim. Change 119 (2), 345–357. https://doi.org/10.1007/s10584-013-0705-8.

Kruger, A.C., Nxumalo, M., 2016. Surface temperature trends from homogenized time series in South Africa: 1931–2015. Int. J. Climatol. 37 (5), 2364–2377. https://doi.org/10.1002/joc.4851.

Kruger, A.C., Nxumalo, M., 2017. Surface temperature trends from homogenized time series in South Africa: 1931–2015. Int. J. Climatol. 37 (5), 2364–2377. https://doi.org/10.1002/joc.4851.

Kruger, A., Sekele, S., 2013. Trends in extreme temperature indices in South Africa: 1962–2009. Int. J. Climatol. 33 (3), 661–676. https://doi.org/10.1002/joc.3455.

Kruger, A.C., Rautenbach, H., Mbatha, S., Ngwenya, S., Makgoale, T.E., 2019. Historical and projected trends in near-surface temperature indices for 22 locations in South Africa. South Afr. J. Sci. 115 (5/6), 1–9. https://doi.org/10.17159/sajs.2019/4846.

Kruger, A.C., Mbatha, S., S, N., 2020. *Trends In Extreme Climate Indices In South Africa*, Pretoria: South African Weather Service. Available at: weathersa.co.za/home/extremeclimateindices.

Kuang, X., Huang, D., Huang, Y., 2021. Inconsistent variation of return periods of temperature extremum in China and its projection based on CMIP6 results. SN Appl. Sci. 3 (12). https://doi.org/10.1007/s42452-021-04863-3.

Lanzante, J.R., 2021. Testing for differences between two distributions in the presence of serial correlation using the <scp>Kolmogorov–Smirnov</scp> and Kuiper's tests. Int. J. Climatol. 41 (14), 6314–6323. https://doi.org/10.1002/joc.7196.

Lee, W., Kim, Y., Sera, F., Gasparrini, A., Park, R., Michelle Choi, H., Prifti, K., Bell, M.L., Abrutzky, R., Guo, Y., Tong, S., De Sousa Zanotti Stagliorio Coelho, M., Nascimento Saldiva, P.H., Lavigne, E., Orru, H., Indermitte, E., Jaakkola, J.J.K., Ryti, N.R.I., Pascal, M., Goodman, P., Zeka, A., Hashizume, M., Honda, Y., Hurtado Diaz, M., César Cruz, J., Overcenco, A., Nunes, B., Madureira, J., Scovronick, N., Acquaotta, F., Tobias, A., Vicedo-Cabrera, A.M., Ragettli, M.S., Guo, Y.-L.L., Chen, B.-Y., Li, S., Armstrong, B., Zanobetti, A., Schwartz, J., Kim, H., 2020. Projections of excess mortality related to diurnal temperature range under climate change scenarios: a multi-country modelling study. Lancet Planet. Health 4 (11), e512–e521. https://doi.org/10.1016/s2542-5196(20)30222-9.

Lim Kam Sian, K.T.C., Hagan, D.F.T., Ayugi, B.O., Nooni, I.K., Ullah, W., Babaousmail, H., Ongoma, V., 2022. Projections of precipitation extremes based on bias-corrected Coupled Model Intercomparison Project phase 6 models ensemble over southern Africa. Int. J. Climatol. https://doi.org/10.1002/joc.7707.

Luber, G., McGeehin, M., 2008. Climate change and extreme heat events. Am. J. Prev. Med. 35 (5), 429–435. https://doi.org/10.1016/j.amepre.2008.08.021.

MacKellar, N., New, M., Jack, C., 2014. Observed and modelled trends in rainfall and temperature for South Africa: 1960-2010. South Afr. J. Sci. 110 (7–8), 1–13. https://doi.org/10.1590/sajs.2014/20130353.

Mafongoya, P., Gubba, A., Moodley, V., Chapoto, D., Kisten, L., Phophi, M., 2019. Climate change and rapidly evolving pests and diseases in southern Africa. New Frontiers in Natural Resources Management in Africa. Natural Resource Management and Policy. Switzerland Springer, Cham. Translated by.

Makunyane, M.S., Rautenbach, H., Sweijd, N., Botai, J., Wichmann, J., 2023. Health risks of temperature variability on hospital admissions in Cape town, 2011–2016. Int. J. Environ. Res. Publ. Health 20 (2), 1159. https://doi.org/10.3390/ijerph20021159.

Maluleke, W., Mokwena, R.J., 2017. The effect of climate change on rural livestock farming: case study of giyani policing area, republic of South Africa. S. Afr. J. Agric. Ext. 45 (1), 26–40. https://doi.org/10.4314/sajae.v45i1.

Mbokodo, I., Bopape, M.-J., Chikoore, H., Engelbrecht, F., Nethengwe, N., 2020. Heatwaves in the future warmer climate of South Africa. Atmosphere 11 (7), 712. https://doi.org/10.3390/atmos11070712.

Mbokodo, I.L., Bopape, M.-J.M., Ndarana, T., Mbatha, S.M.S., Muofhe, T.P., Singo, M.V., Xulu, N.G., Mohomi, T., Ayisi, K.K., Chikoore, H., 2023. Heatwave variability and structure in South Africa during summer drought. Climate 11 (2), 38. https://doi.org/10.3390/cli11020038.

McBride, C.M., Kruger, A.C., Dyson, L., 2021. Trends in probabilities of temperature records in the non-stationary climate of South Africa. Int. J. Climatol. https://doi.org/10.1002/joc.7329.

Meinshausen, M., Smith, S.J., Calvin, K., Daniel, J.S., Kainuma, M.L.T., Lamarque, J.F., Matsumoto, K., Montzka, S.A., Raper, S.C.B., Riahi, K., Thomson, A., Velders, G.J.M., Van Vuuren, D.P.P., 2011. The RCP greenhouse gas concentrations and their extensions from 1765 to 2300. Clim. Change 109 (1–2), 213–241. https://doi.org/10.1007/s10584-011-0156-z.

Morrison, S.R., 1983. Ruminant heat stress: effect on production and means of alleviation. J. Anim. Sci. 57 (6). https://doi.org/10.2527/jas1983.5761594x.

Nangombe, S.S., Zhou, T., Zhang, W., Zou, L., Li, D., 2019. High-temperature extreme events over Africa under 1.5 and 2 °C of global warming. J. Geophys. Res. Atmos. 124 (8), 4413–4428. https://doi.org/10.1029/2018jd029747.

New, M., Hewitson, B., Stephenson, D.B., Tsiga, A., Kruger, A., Manhique, A., Gomez, B., Coelho, C.A.S., Masisi, D.N., Kululanga, E., Mbambalala, E., Adesina, F., Saleh, H., Kanyanga, J., Adosi, J., Bulane, L., Fortunata, L., Mdoka, M.L., Lajoie, R., 2006. Evidence of trends in daily climate extremes over southern and west Africa. J. Geophys. Res. 111 (D14). https://doi.org/10.1029/2005jd006289.

Ng, J.L., Chan, K.H., Md Noh, N.I.F., Razman, R., Surol, S., Lee, J.C., Al-Mansob, R.A., 2022. Statistical modelling of extreme temperature in Peninsular Malaysia. IOP Conference Series: Earth and Environmental Science. IOP Publishing, 012072.

Nguyen, P.L., Alexander, L.V., Thatcher, M.J., Truong, S.C.H., Isphording, R.N., McGregor, J.L., 2024. Selecting CMIP6 global climate models (GCMs) for Coordinated Regional Climate Downscaling Experiment (CORDEX) dynamical downscaling over Southeast Asia using a standardised benchmarking framework. Geosci. Model Dev. (GMD) 17 (19), 7285–7315. https://doi.org/10.5194/gmd-17-7285-2024.

Olabanji, M.F., Ndarana, T., Davis, N., 2020. Impact of climate change on crop production and potential adaptive measures in the olifants catchment, South Africa. Climate 9 (1), 6. https://doi.org/10.3390/cli9010006.

Rader, R., Reilly, J., Bartomeus, I., Winfree, R., 2013. Native bees buffer the negative impact of climate warming on honey bee pollination of watermelon crops. Glob. Change Biol. 19 (10), 3103–3110. https://doi.org/10.1111/gcb.12264.

Rosenzweig, C.E., Iglesias, A., Yang, X.B., Epstein, P.R., Chivian, E., 2001. Climate change and extreme weather events - implications for food production, plant diseases, and pests. Global Change Hum. Health 2 (2).

Rotstayn, L.D., Collier, M.A., Jeffrey, S.J., Kidston, J., Syktus, J.I., Wong, K.K., 2013. Anthropogenic effects on the subtropical jet in the southern Hemisphere: aerosols versus long-lived greenhouse gases. Environ. Res. Lett. 8. https://doi.org/10.1088/1748-9326.

Saddique, N., Khaliq, A., Bernhofer, C., 2020. Trends in temperature and precipitation extremes in historical (1961–1990) and projected (2061–2090) periods in a data scarce mountain basin, northern Pakistan. Stoch. Environ. Res. Risk Assess. 34 (10), 1441–1455. https://doi.org/10.1007/s00477-020-01829-6.

Sarr, A.B., Diba, I., Basse, J., Sabaly, H.N., Camara, M., 2019. Future evolution of surface temperature extremes and the potential impacts on the human health in Senegal. Afr. J. Environ. Sci. Technol. 13 (21), 482–510. https://doi.org/10.5897/ajest2019.2757.

Schumann, E.H., Martin, J.A., 1991. Climatological aspects of the coastal wind field at Cape town, Port Elizabeth and durban. S. Afr. Geogr. J. 73 (2), 48–51. https://doi.org/10.1080/03736245.1991.9713548.

Serdeczny, O., Adams, S., Baarsch, F., Coumou, D., Robinson, A., Hare, W., Schaeffer, M., Perrette, M., Reinhardt, J., 2017. Climate change impacts in Sub-Saharan Africa: from physical changes to their social repercussions. Reg. Environ. Change 17 (6), 1585–1600. https://doi.org/10.1007/s10113-015-0910-2.

Singo, M.V., Chikoore, H., Engelbrecht, F.A., Ndarana, T., Muofhe, T.P., Mbokodo, I.L., Murungweni, F.M., Bopape, M.-J.M., 2023. Projections of future fire risk under climate change over the South African savanna. Stoch. Environ. Res. Risk Assess. 37 (7), 2677–2691. https://doi.org/10.1007/s00477-023-02412-5.

Soares, P.M.M., Careto, J.A.M., Cardoso, R.M., Goergen, K., Trigo, R.M., 2019. Land-atmosphere coupling regimes in a future climate in Africa: from model evaluation to projections based on CORDEX-africa. J. Geophys. Res. Atmos. 124 (21), 11118–11142. https://doi.org/10.1029/2018jd029473.

Thornton, P., Nelson, G., Mayberry, D., Herrero, M., 2021. Increases in extreme heat stress in domesticated livestock species during the twenty-first century. Glob. Change Biol. 27 (22), 5762–5772. https://doi.org/10.1111/gcb.15825.

Tjiputra, J.F., Roelandt, C., Bentsen, M., Lawrence, D.M., Lorentzen, T., Schwinger, J., Seland, Ø., Heinze, C., 2013. Evaluation of the carbon cycle components in the Norwegian earth system model (NorESM). Geosci. Model Dev. (GMD) 6 (2), 301–325. https://doi.org/10.5194/gmd-6-301-2013.

Turasie, A.A., 2021. Exceedance and return period of high temperature in the african region. Climate 9 (53). https://doi.org/10.3390/cli9040053.

Van Der Walt, A.J., Fitchett, J.M., 2021. Exploring extreme warm temperature trends in South Africa: 1960–2016. Theor. Appl. Climatol. https://doi.org/10.1007/s00704-020-03479-8.

Van Vuuren, D.P., Edmonds, J., Kainuma, M., Riahi, K., Thomson, A., Hibbard, K., Hurtt, G.C., Kram, T., Krey, V., Lamarque, J.-F., Masui, T., Meinshausen, M., Nakicenovic, N., Smith, S.J., Rose, S.K., 2011. The representative concentration pathways: an overview. Clim. Change 109 (1–2), 5–31. https://doi.org/10.1007/s10584-011-0148-z.

Voldoire, A., Sanchez-Gomez, E., Salas Y Mélia, D., Decharme, B., Cassou, C., Sénési, S., Valcke, S., Beau, I., Alias, A., Chevallier, M., Déqué, M., Deshayes, J., Douville, H., Fernandez, E., Madec, G., Maisonnave, E., Moine, M.P., Planton, S., Saint-Martin, D., Szopa, S., Tyteca, S., Alkama, R., Belamari, S., Braun, A., Coquart, L., Chauvin, F., 2013. The CNRM-CM5.1 global climate model: description and basic evaluation. Clim. Dyn. 40 (9–10), 2091–2121. https://doi.org/10.1007/s00382-011-1259-y.

Warnatzsch, E.A., Reay, D.S., 2019. Temperature and precipitation change in Malawi: evaluation of CORDEX-Africa climate simulations for climate change impact assessments and adaptation planning. Sci. Total Environ. 654, 378–392. https://doi.org/10.1016/j.scitotenv.2018.11.098.

Watanabe, S., Hajima, T., Sudo, K., Nagashima, T., Takemura, T., Okajima, H., Nozawa, T., Kawase, H., Abe, M., Yokohata, T., Ise, T., Sato, H., Kato, E., Takata, K., Emori, S., Kawamiya, M., 2011. MIROC-ESM 2010: model description and basic results of CMIP5-20c3m experiments. Geosci. Model Dev. (GMD) 4 (4), 845–872. https://doi.org/10.5194/gmd-4-845-2011.

Wichmann, J., 2017. Heat effects of ambient apparent temperature on all-cause mortality in Cape Town, Durban and Johannesburg, South Africa: 2006–2010. Sci. Total Environ. 587–588, 266–272. https://doi.org/10.1016/j.scitotenv.2017.02.135.

Wilks, D.S., 2011. Statistical Methods in Atmospheric Sciences. Academic press.

Xu, J., Gao, Y., Chen, D., Xiao, L., Ou, T., 2017. Evaluation of global climate models for downscaling applications centred over the Tibetan Plateau. Int. J. Climatol. 37 (2), 657–671. https://doi.org/10.1002/joc.4731.

Xu, Y., Gao, X., Giorgi, F., Zhou, B., Shi, Y., Wu, J., Zhang, Y., 2018. Projected changes in temperature and precipitation extremes over China as measured by 50-yr return values and periods based on a CMIP5 ensemble. Adv. Atmos. Sci. 35 (4), 376–388. https://doi.org/10.1007/s00376-017-6269-1.

Xu, Z., Han, Y., Tam, C.-Y., Yang, Z.-L., Fu, C., 2021. Bias-corrected CMIP6 global dataset for dynamical downscaling of the historical and future climate (1979–2100). Sci. Data 8 (1). https://doi.org/10.1038/s41597-021-01079-3.

Yeon-Hee, Kim, Seung-Ki, Min, Xuebin, Zhang, Jana, Sillmann, Marit, Sandstad, 2020. Evaluation of the CMIP6 multi-model ensemble for climate extreme indices. Weather Clim. Extrem. 29. https://doi.org/10.1016/j.wace.2020.100269.

Zhu, X., Troy, T.J., 2018. Agriculturally relevant climate extremes and their trends in the world's major growing regions. Earths Future 6 (4), 656–672. https://doi.org/10.1002/2017ef000687.

Ziervogel, G., Zermoglio, F., 2009. Climate change scenarios and the development of adaptation strategies in Africa: challenges and opportunities. Clim. Res. 40, 133–146. https://doi.org/10.3354/cr00804.

Ziervogel, G., Lennard, C., Midgley, G., New, M., Simpson, N.P., Trisos, C.H., Zvobgo, L., 2022. Climate change in South Africa: risks and opportunities for climate-resilient development in the IPCC Sixth assessment WGII report. South Afr. J. Sci. 118 (9/10). https://doi.org/10.17159/sajs.2022/14492.

Zwiers, F.W., Zhang, X., Feng, Y., 2011. Anthropogenic influence on long return period daily temperature extremes at regional scales. J. Clim. 24 (3), 881–892. https://doi.org/10.1175/2010jcli3908.1.